ANALYSIS OF THE HISTONE METHYLTRANSFERASE ASH2L VIA RNA INTERFERENCE AND CRISPR-CAS9 DURING BOVINE EARLY EMBRYONIC DEVELOPMENT

A Thesis

by

MATTHEW D SNYDER

Submitted to the Office of Graduate and Professional Studies of
Texas A&M University
in partial fulfillment of the requirements for the degree of

MASTER OF SCIENCE

Committee Chair,	Charles R. Long
Committee Members,	Mark E. Westhusin
	Michael C. Golding
	Carey Satterfield
Head of Department,	Larry J. Suva

August 2016

Major Subject: Biomedical Sciences

Copyright 2016 Matthew Snyder

ABSTRACT

Epigenetic patterns established during early bovine embryogenesis via DNA methylation and histone modification patterns are essential for proper gene expression and embryonic development. Epigenome patterns established during this period, if improperly maintained, can lead to developmental anomalies and may partially explain the lower pregnancy rates of in vitro-produced embryos. We hypothesized that the histone methyltransferase of ASH2L would alter preimplantation development, epigenetic reprogramming, and gene expression profiles in the early bovine embryo. We observed that the depleted and deleted ASH2L embryos developed to the blastocyst stage with suppressed ASH2L having comparable development rates with its respective control (31.3 ± 2.0%, n = 466 v. 34.8 ± 1.9%, n = 418). To see if errors were in the chromatin structure at the blastocyst stage, DNA methylation and histone modifications were examined to further explain the role of ASH2L during embryonic development. Blastocysts from each treatment (N = 601) were fixed and prepared for immunocytochemistry following standard laboratory protocol. Our findings show ASH2L may play a role in DNA methylation by decreasing 5mc and 5hmc conversion, which is a key event during early embryonic development. Suppression of ASH2L also alters global levels of H3H4me3 and H3K27me3 ($p<0.001$), which may lead to transcription aberrations. RNA-seq showed altered gene expression profiles in 407 genes in the morphologically comparable Day 17 conceptus ($p<0.05$). Closer examination showed that there is altered mesenchymal stem cell differentiation present in the Day 17 conceptuses. Analysis of ASH2L shows to not have a detrimental effect during

preimplantation development but altered chromatin status and gene expression profiles suggest that ASH2L could play a vital role later in development.

DEDICATION

I wish to dedicate this thesis to my family and friends that
have supported me throughout my graduate studies.

To my father:
Thank you for all of your support during my graduate studies,
showing me that hard work can go a long ways,
and for taking care of my cows during my time in Texas.

To my sister:
For all of your encouragement to continue my education
and for being a great role model over the years.

And to my fiancée:
Thank you for your continued patience,
support throughout my graduate studies,
and words of encouragement along the way.

ACKNOWLEDGEMENTS

I would like to thank Dr. Charles Long for giving me the opportunity to pursue my research at Texas A&M. I am amazed by all of the excellent learning opportunities that I have experienced during my graduate studies. I would also like to thank my committee members Dr. Mark Westhusin, Dr. Michael Golding, and Dr. Carey Satterfield for their advice and support along the way.

Furthermore, I would like to thank Jane Pryor for her mentorship and guidance with IVF and micromanipulation of embryos. Without your guidance I would not be where I am at today. I would like to also thank current and past graduate students in the IVF lab (Michael Peoples and Carlos Pinzon) for their many hours of help on this project.

I would like to thank current and past members at the Reproductive Sciences Lab (Dr. Neetu Singh, Dr. Lisbeth Ramirez-Carvajal, Hanah Georges, William Skiles, and Dr. Kylee Veazey) for all of your help and mentorship with aspects of CRISPR-Cas9, RNA-seq, and RT-qPCR. I would also like to thank other members at the lab for being excellent colleagues and friends along the way.

Finally, I would like to thank the National Institutes of Health (Eunice Kennedy Shriver National Institute for Child Health and Human Development, Grant No. 5R01HDO58969-04) and the Texas A&M University College of Veterinary Medicine (2014 Biomedical Sciences CVM Graduate Student Training Grant) for the funding that helped make this research possible.

NOMENCLATURE

5hmc	5-hydoxymethylcystosine
5mc	5-methylcytosine
Amp	Ampicillin
ARTs	Assisted reproductive technologies
AS	Angelman Syndrome
bp	Base pairs
BWS	Beckwith-Wiedemann Syndrome
cDNA	Complementary DNA
ChIP	Chromatin histone immunoprecipitation
CIDR	Controlled internal drug release
CL	Corpus luteum
CpG	Cytosine-Guanine (dinucleotides)
CRISPR	Clustered regularly-interspaced short palindromic repeats
DNMTs	DNA methyltransferases
dsRNA	Double-stranded RNA
FBS	Fetal bovine serum
H3K4	Histone 3 Lysine 4
H3K9	Histone 3 Lysine 9
H3K27	Histone 3 Lysine 27
HMTs	Histone methyltransferases
HOX	Homeobox

ICC	Immunocytochemistry
IFNT	Interferon tau
InDels	Insertion or deletions
IVC	In vitro culture
IVF	In vitro fertilization
IVM	In vitro maturation
IVP	In vitro produced
IVT	In vitro transcription
NHEJ	Nonhomologous end joining
LOS	Large offspring syndrome
MDBK	Madin-Darby bovine kidney
me2	Dimethylation
me3	Trimethylation
MLL	Mixed Lineage Leukemia
mRNA	Messenger RNA
PAM	Protospacer adjacent motif
PcG	Polycomb group
PCR	Polymerase chain reaction
PHD	Plant homeodomain
Puro	Puromycin
RISC	RNA induced silencing complex
RNAi	RNA interference
RT-qPCR	Real-time quantitative PCR

SCNT	Somatic cell nuclear transfer
Seq	Sequencing
siRNA	small interfering RNA
sgRNA	small guide RNA
SPRY	SPIa/RYanodine receptor
TrxG	Trithorax Group
TSS	Transcription start sites

TABLE OF CONTENTS

Page

Page

LIST OF FIGURES

Figure Page

LIST OF TABLES

CHAPTER I

INTRODUCTION

Assisted Reproductive Technologies in Cattle and Humans

With the introduction of the first *in vitro* produced bovine calf in 1981, *in vitro* fertilization (IVF) has become an increasingly utilized technique within the bovine embryo transfer industry [1]. Assisted reproductive technologies (ARTs) that produce embryos outside of the *in vivo* environment include *in vitro* maturation (IVM), IVF, and *in vitro* culture (IVC). When these technologies are combined the embryos are often refered to as *in vitro* produced (IVP). IVP is a useful method that producers can incorporate into their business to increase offspring from superior cattle at a faster rate when compared to *in vivo* production. The attraction to this technique is demonstrated by the reported 443,533 bovine IVP embryos in 2013 (IETS Statistics, 2013). When compared to five years earlier, there is a substantial increase as only 245,260 embryos were reported from IVP techniques (IETS Statistic, 2008). Over this period, there was also an increased proportion of IVP embryos being transferred into recipients (38.8% vs 29.7%; IETS Statistics, 2013 & 2008 respectively).

As *in vitro* technologies began to be commercialized, these IVP embryos resulted in inferior pregnancy rates (56% fresh and 42% frozen) when compared to their *in vivo* counterparts derived from superovulation and embryo transfer (76% fresh and 64% frozen) [2]. In a more recent examination of the industry, lower pregnancy rates were still present on Day 30 (32% vs 46%) and Day 60 (27% vs 42%) [3]. Additional studies support this decrease in pregnancy on Day 60 when comparing the *in vitro* and *in vivo* produced embryos

(33.5% verse 41.2%, respectively) [4]. These decreased pregnancy rates suggest IVP embryos are developmentally inferior and improvements are necessary in culture systems in order to optimize embryo quality and pregnancy rates [5].

Altered development rates were further highlighted with the increase use of somatic-cell nuclear transfer (SCNT) in cattle. It was shown that cloned fetuses had increased abortion rates during pregnancy, with viability being reported as low as 10% on Day 180 [6]. Failure in normal placentation was found to be the major cause of this failure in pregnancy [7]. The small percent of fetuses from SCNT survived through gestation sometimes exhibited phenotypic anomalies at birth. It was observed that cloned fetuses resulted in an approximate 20% increase in birth weight when compared to calves from embryo transfer and artificial insemination. This phenomenon became commonly known as large offspring syndrome (LOS). LOS calves also presented multiple health issues that were believed to be caused by cloning techniques and *in vitro* culture conditions [8, 9]. These abnormal calves from SCNT were also found to have abnormal gene expression patterns of developmentally important genes that lead to the altered physiological and phenotypic variation from the *in vivo* offspring [10, 11]. These findings in bovine provide insight for other species, including humans, that have similar phenotypic anomalies in offspring associated with ARTs.

In humans, there is increase use of ARTs since the first IVF baby born in 1978. In 2013, more than 1.5% (63,286) of children were reported to be born in the United States from these techniques. However, there were also numerous failed instances of producing a viable offspring from ARTs, with a reported 111,676 (63.8%) attempts being unsuccessful (2013 Fertility Clinic Report, CDC). With the average age of the human reproductive population increasing, there is a projected decrease in fertility. This suggests ARTs will be a

more commonly used technique in the future [12]. With the reported large number of failed IVF attempts in humans, it suggests errors are present in gene expression patterns of these early embryos [13, 14]. Similar to observations of LOS in cattle and sheep; ARTs in humans have also been linked to imprinting disorders Beckwith-Wiedemann Syndrome (BWS) and Angelman Syndrome (AS) [15, 16]. Children born with BWS are reported to be overweight and have atypical phenotypes present at birth. Children with BWS are also more prevalent to tumorigenesis and other health risks throughout life [17]. With the mounting evidence of epigenetic errors present in these offspring, it is important to investigate factors present during *in vitro* culture that cause abnormal embryonic development [18].

These findings from ARTs in both humans and cattle offspring have led researchers to take a closer look at gene expression profiles of IVP embryos and the subsequent offspring [19]. It has been shown in mice that abnormal regulation of genomic imprinting regions were present due to different *in vitro* culture mediums being utilized [20]. Epigenetic disruption to imprinted genes has previously been identified as a potential mechanism that leads to the abnormal placentation, and thus, phenotypic difference for LOS, BWS, and AS. Further investigation of IVP embryos in cattle discovered a large proportion of embryos exhibited errors in gene expression profiles when compared to *in vivo* produced embryos [21]. Later studies used deep transcriptome analysis further validated these differenes in gene expression between the *in vitro* and *in vivo* produced embryos. These anomalies associated with ARTs shows a need for better culture systems in order to facilitate fertilization without the detrimental side effects.

Epigenetics

Epigenetics means "above genetics" and refers to DNA methylation and/or histone modifications that regulate transcription [22]. These modifications do not alter the underlying DNA sequence, but instead influence transcription by alterations in chromatin structure. It was believed for the majority of the twentieth century that genetics, environment, and developmental biology were entirely separate fields [23]. It was not until the 1960s, the science of epigenetics established a link between these fields [24]. Due in part to technical advances in analysis of chromatin components, a vast amount of research has been accomplished to characterize epigenetic regulation of the genome.

Epigenetic regulation can come in the form of DNA methylation and/or histone modifications. The modifications that occur during early embryonic development can be heritable to subsequent daughter cells in the lineage [25]. These modifications help to shape the developmental plan from the zygote stage and throughout development. Substantial, research has focused on environmental factors present *in vitro* and how they may effect the establishment of DNA methylation and histone modification patterns of the early embryo [26]. With the increase use of *in vitro* embryo production in both humans and livestock species, research into epigenetic patterns is important in order to understand chromatin remodeling of the early embryo. Moreover, how these perturbations to the chromatin may lead to subsequent manifestation of abnormal phenotypes associated with ARTs.

DNA Methylation and Hydroxymethylation

DNA methylation is an epigenetic mechanism that can be used to modulate the transcriptional status of mammalian cells. DNA methylation has been associated with playing

a vital role in transcription, chromatin structure, genomic imprinting, embryonic development, and chromatin stability [27-30]. Of the different types of DNA methylation, the fifth carbon position of cytosine (5mc) has been popularly studied and is shown to be inherited through somatic cell division [31, 32]. Thus far, most studies examining DNA methylation have focused on CpG islands [33, 34]. CpG islands are regions of the DNA where a cytosine nucleotide is followed by a guanine nucleotide and are typically located near the transcription start sites (TSS) of genes. Cytosine methylation at the CpG sites in promoter regions are often associated with a decrease in transcriptional activity due to inhibition of the binding of RNA polymerase, thus inhibiting gene transcription [35, 36]. However, this is not always true as it has been shown that 5mc levels have been associated with both a positive and negative correlation on regulating gene transcription [37].

The DNA methyltransferases (DNMTs), are a conserved family of proteins that play a key role in DNA methylation and are considered to be necessary for mammalian development [38]. DNMT1 is considered to be maintenance protein as it is responsible for passing on the methylation patterns from the dividing cells onto daughter cells in order to maintain chromatin stability [39]. DNMT3a and DNMT3b play a pivotal role in *de novo* methylation and establishing 5mc levels in primordial germ cells and during preimplantation development [40].

During the preimplantation stage, global DNA methylation patterns play a valuable role in epigenetic reprogramming in most mammalian species (Figure 1.1) [41, 42]. Shortly after fertilization, the paternal and maternal genome undergo asymmetrical demethylation patterns that converts 5mc to 5-hydroxymethylcytosine (5hmc) [43-46]. Hydroxymethylation in 5mc in the early embryo is mediated by the enzymes of ten-eleven translocation 1 (TET1),

TET2, and TET3 [47, 48]. In mice, suppression of TET1 in the early embryo resulted in a bias towards trophectoderm differentiation [49]. These findings in mice suggest that 5hmc plays a role in differentiation and proper gene expression profiles in the early embryo. However, examples in sheep and cloned embryos, from a variety of species, proved that this methylation pattern is not always essential for embryo viability [42, 50, 51].

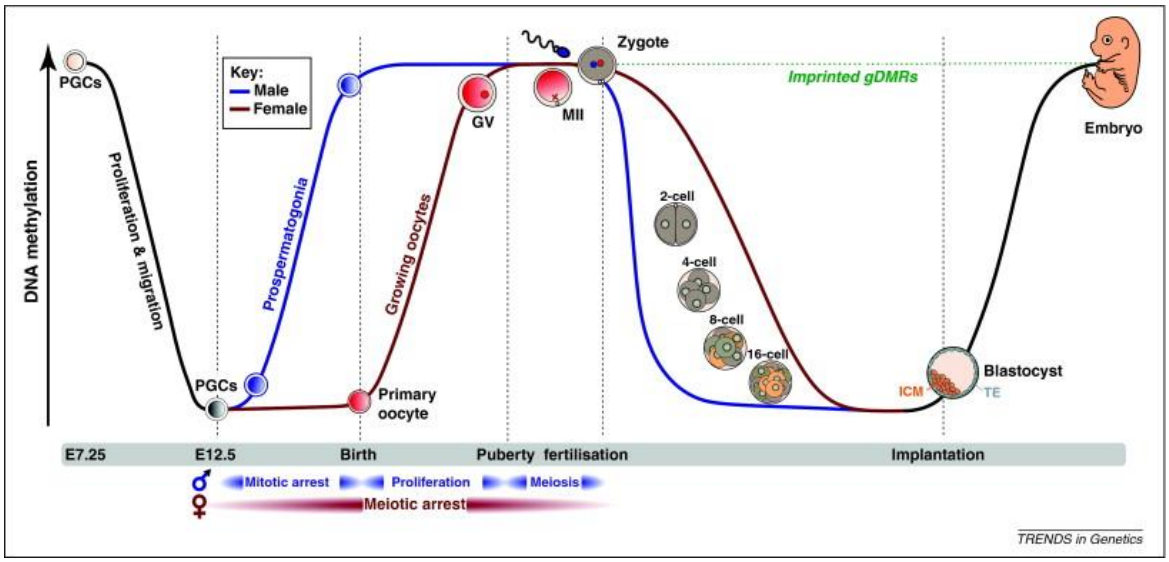

Figure 1.1 – DNA methylation patterns in primordial germ cells and early embryo in mice [41].

5mc and 5hmc patterns established during the early stages of preimplantation development are thought to be a necessary for viability of the early embryo [52]. After fertilization the early stages in embryo development are controlled by maternal mRNA and proteins. Genome activation is needed in the early embryo for it to synthesize new protein and thus allowing further cleavage stages to take place [53]. During this reprogramming

event, DNA methylation has been shown to associate with chromatin modifiers to aid in this reprogramming process.

Imprinted genes have been shown to bypass regular DNA methlylation patterens present in the early embryo [54]. Imprinted genes were first discovered in mice and it was revealed that it was required for both the paternal and maternal allele to create a viable embryo [55]. These allele specific patterns have been shown to be improperly maintained by epigenetic factors that give rise to abnormal phenotypes that are associated with ARTs [56,57]. Ambnormal regulation of imprinting genes has been shown to be the problem with loss of imprinting and abnormal placentaion during fetal development [58,59]. Finding the epigenetic factors that cause this abnormal regulation of imprinting genes in the early embryo would be beneficial for future development.

Histone Modifications

In 1964, it was first discovered that acetylation and methylation of core histone proteins are associated with changes in RNA synthesis [60]. Two copies each of the core histone proteins of H2A, H2B, H3 and H4 aid in packaging DNA and together form the nucleosome [61]. The DNA wrapped around these histones are approxamitaly 147 base pairs (bp) long, while linker DNA connects the histones to one another [62]. Histone modifications take place on these core proteins are associated with facilitating gene transcription based on the accessibility of the chromatin [63]. Modifications to histone tails are key regulators for chromtin assembly and transcriptional activity [64]. The most commonly studied modifications to histone tails include methylation, phosphorylatin, acetylation, and ubiquitation [65].

Histone methyltransferases (HMTs) are key components of epigenetic reprogramming, as they are associated with the initiation of gene expression [66]. Many different mechanisms are found to play a role in this process. Some of these histone methylation sites include, but are not limited to, histone 3 lysine 4 (H3K4), H3K9, H3K20, H3K27, H3K36, and H3K79. Methylation of H3K4, H3K36 and H3K79 have been associated with a more acitve chromatin while H3K9 and H3K27 have been associated with transcriptionally repressed chromatin [67,68]. The methylation on the histone tails can be quite specific as it can be mono-, di-, and tri-methylated, with trimethylation generally having the most substantial effect on regulation of gene expression [69].

Two major protein groups, the Trithorax group (TrxG) and Polycomb group (PcG), aid in maintating the methylation status on histone tails and are associated with playing a role in the cell cycle (Figure 1.2) [70]. The TrxG and PcG of proteins are also able to exchange their binding sites with histones multiple times throughout cell divisions, thus showing histone modifications can be erased and re-established [71]. In general, the TrxG of proteins are associated with leaving the chromatin more accessible for gene transcription while the PcG of proteins has an inverse function.

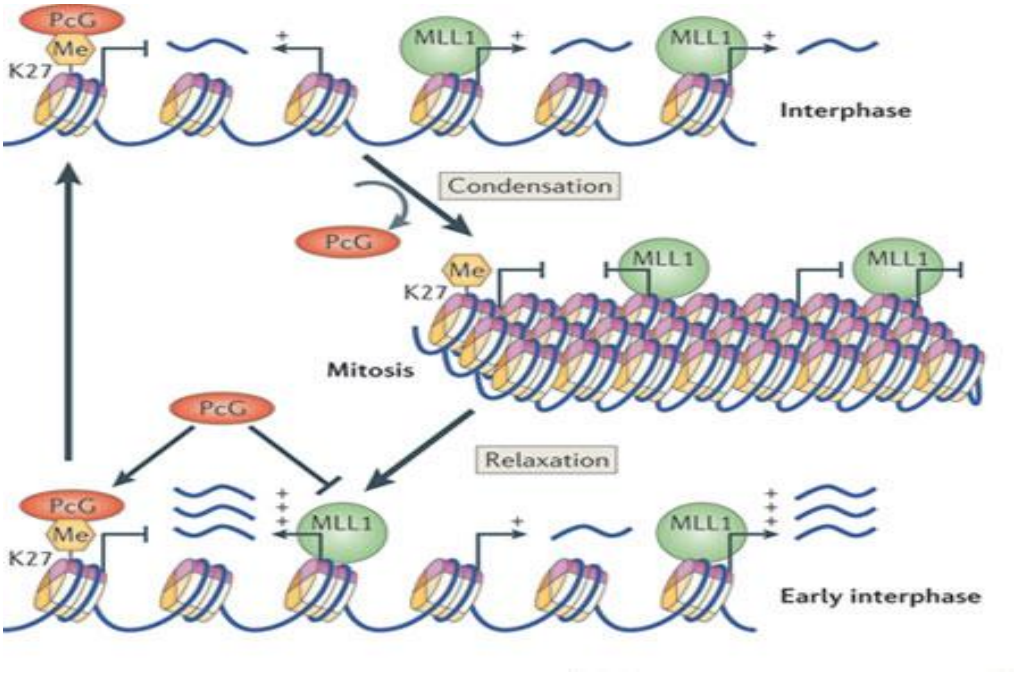

Figure 1.2 – Overview of the role of Mixed Lineage Luekemia 1 (MLL1) on chromatin remodeling. MLL1 is a component of Trithorax Group, and Polycomb Group (PcG) role during the cell cycle and how they exchange their binding sites with histones multiple times throughout cell division. The resulting effect is condensation and relaxation of the chromatin [70].

The TrxG and PcG proteins work together to regulate Homeobox (HOX) genes expression during early embryonic development. Regulation of H3K4 by the TrxG and H3K27 by the PcG is critical for HOX gene expression and the layout of developmental plan for the early embryo [72]. Abnormal HOX gene expression has been linked to atypical development throughout the body including skeletal, reproductive, and digestive systems [73,74]. To date, the majority of studies investigating the role of histone methylation on the control of HOX gene expression and other histone modifications have been completed by using a mouse model [75].

Biomedical Animal Models

The majority of studies of epigenetic modifications during the preimplantation period have used the mouse as the mammalian model. However, differences in terms of epigenetic reprogramming and epigenetic regulation of gene expression between species is apparent [76]. Therefore, defining key epigenetic modifiers during preimplantation development in bovine is valuable as they are a biologically more relevant model to the human as compared to the mouse [77]. Cattle are also an economically important livestock species where ARTs are often used, making bovine studies relevant in human medicine and agricultural industries.

Reproductively, the mouse has a shorter preimplantation and gestational period (21 days) when compared to humans (280 days). Cattle are more similar to humans in gestational length (approximately 282 days, depending on breed) [78]. During preimplantation development, there are noticeable differences in embryo development when comparing humans to mice and cattle. Mice reach the blastocyst stage of embryonic development on Day 3.5 as compared to humans and bovine (Day 5-6 and Day 6-7 respectively) [79]. Embryonic genome activation also varies between the mammalian species as the mouse genome activation occurs at the two-cell, humans begin at the four-cell stage, and bovine at the 8-16 cell stage [80]. It has also been shown that the bovine genome is more comparable in alignment to human genome than mice [81, 82].

With over 95% of studies analyzing gene function occurring in mice, utilizing animal models that are genetically more similar to humans would be beneficial [83]. Utilizing the bovine as a research model can benefit the cattle industry as well as providing a better understanding of epigenetic regulation, which could help increase pregnancy rates and decrease disease pathogenesis that are associated IVP embryos. With the increase use of IVP

and commercially available oocytes in cattle, this further makes the bovine an attractive research model.

Tools for Studying Functional Genomics

RNA Interference

RNA interference (RNAi) is an evolutionarily conserved mechanism that has been associated with modulating gene expression in eukaryotes. RNAi was first discovered in plant species and was found to play a role in translational repression by post-transcriptional gene siliencing [84]. It was later shown that double stranded RNA (dsRNA) caused the silencing of the targeted genes [85]. The use of RNA interference can target specific RNA sequences with high specificity base pairing. This is achieved in mammalian cells by long dsRNA that are cleaved, by the enzyme Dicer, into short double-stranded RNA that are approximately 21 to 26 nucleotides long [86]. This RNA induced silencing complex (RISC) contains two single-stranded RNAs that consist of a guide strand and a passenger strand that results in the passenger strand binding to a specific sequence of the mRNA [87]. Gene silencing by RISC is achieved by three different mechanisms: homology dependent mRNA degradation, translational suppression, or transcriptional gene silencing [88]. This can be utilized in cells and embryos by delivering double stranded siRNAs to a specific sequence to mediate post-transcriptional silencing and achieve reduction of protein [89].

CRISPR-Cas9

The type II prokaryotic clustered regularly-interspaced short palindromic repeats (CRISPR) when combined with the DNA endonuclease enzyme Cas9 has been shown to be

effective for precise genome editing in mammalian cells [89]. CRISPR-Cas9 is a bacterial adaptive immune system that has been engineered to function in eukaryotic cells in a quick, efficient, and low cost manner [90]. It can be designed to target a specific location to disrupt gene function with a Cas9 enzyme and a 20 base pair guide RNA target sequence adjacent to a PAM site (3' NGG). After the guide RNA aligns the Cas9 enzyme to a specific sequence, Cas9 will recognize the PAM site and perform a double strand break. The double strand break is then repaired by nonhomologous end joining (NHEJ); an error prone repair mechanism that frequently causes insertion or deletions (InDels) in the DNA. These InDels will likely cause a frameshift mutation in the coding sequence, thus disrupting the function of the gene. It has been shown that CRISPR/Cas9 can have a wide array of functions from knockout and insertion of certain gene sequences to repair mutations [91, 92]. This wide spread high specificity is useful for analyzing the function for different genes. Since the result is the loss of gene function, it is also an effective tool for analyzing gene function in the early embryo [93].

Bovine Uterine Environment for Transfer and Collection

In vitro embryo culture systems can only support the development of the bovine embryo until shortly after the blastocyst embryo is hatched out of the zona pellucida. After this point in time, the embryo requires an *in vivo* environment for continuation of development. In bovine, there is a period of development after the blastocyst stage where the embryo undergoes rapid elongation before attaching to the endometrial cells of the uterus [94]. The initiation of elongation of the blastocyst occurs on Day 12 to 14 in bovine. In the uterine environment, progesterone works to stimulate blastocyst growth and elongation

during this pre-implantation period [95-97]. The elongation of the trophectoblast cells is critical for the for the release of interferon tau (IFNT) for maternal recognition of pregnancy in cattle [98]. If an insufficient quantity of IFNT is produced, PGF2-alpha will be released to lyse the corpus lutea and thus contining the estrus cycle.

Embryos require transfer into estrus synchronized recipients in order to replicate the uterine environment for the Day 7 embryos [99]. Estrous synchronization protocols are common in the embryo transfer industry, with the standard CIDR method being used for timed embryo transfer [100]. In order to avoid surgical procedures on recipient females, embryos can be collected on Day 17 of development [101]. On Day 17 embryo elongates into a long filamentous conceptus to contains a small embryonic disc [102]. On Day 19 the elongated bovine conceptus will begin binding to the uterine epithelium [103]. Once this binding begins, conventional nonsurgical embryo collection would no longer be possible for examination of the conceptus. Later in development, the elongated filamentous trophectoderm will become the placenta, while the embryonic disc will develop into the fetus. In previous studies, it has been shown that transferring of up to eleven embryos per recipient can be achieved while still maintaining elongation and embryo viability [104]. Collection of conceptuses at this time allows for non-invasive techniques to the recipient that will allow her to be used for future experiments.

Epigenetic Modifiers in Bovine Embryos

DNMTs and HMTs have previously been studied in bovine preimplantation embryos by using a RNA interference approach [105-109]. All of the genes studied, when suppressed in the early embryo, have had an inhibitory effect on preimplantation development up to the

blastocyst stage (Table 1.1). Due to morphological and developmental changes caused by the suppression of the DNMTs and HMTs, analysis of ASH2L will give valuable information on its role during preimplantation development in bovine. Furthermore, no member of the TrxG of proteins has yet to be analyzed for their role during bovine preimplantation development.

DNA Methyltransferases	Histone Methyltransferases
DNMT1	SUZ12
DNTM3A	SMYD3
DNTM3B	EHMT2 (G9A)
LSH	SETDB1
	SUV3-9H1
	SUV4-20H1

Table 1.1 – DNMTs and HMTs previously studied during bovine preimplantation development.

Ash2 (Absent, Small, and Homeotic)-Like (ASH2L)

Ash2 was first discovered in Drosophila and was determined to belong to the TrxG gene family as a positive regulator of gene expression. The ASH2L protein is a known HMT that plays a role in H3K4 [110]. ASH2L is also a core component of the Trithorax group of proteins, also known as the Mixed Lineage Leukemia (MLL) protein. The Trithorax group is a multiprotein complex that requires the presence of ASH2L, WD Repeat Domain 5 (WDR5), Retinoblastoma Binding Protein 5 (RBBP5), Dpy-30 Histone Methyltransferase Complex Regulatory Subunit (DPY30) and Host Cell Factor (HCF) proteins in order for the

complex to be in an active state [111]. Its interaction with RBBP5 is necessary for complex integrity and activity regulation [112]. The binding of ASH2L to DPY30 is important for the regulation of the trimethylation of H3K4 [113, 114].

This active state could be a key factor in the epigenetic reprogramming as it is a member of the MLL complex that regulates the methylation of the histone H3 Lysine 4 (H3K4) and facilitates the chromatin to be more accessible for transcription [115, 116]. It has been shown that trimethylation of H3K4 is associated with active gene transcription and thus plays a role in developmental regulation. If improperly maintained it can lead to disease pathogenesis, including cancer in mammals [117]. ASH2L and the trimethylation of H3K4 are associated with increased transcription of HOX genes (Figure 1.3) [118, 119].

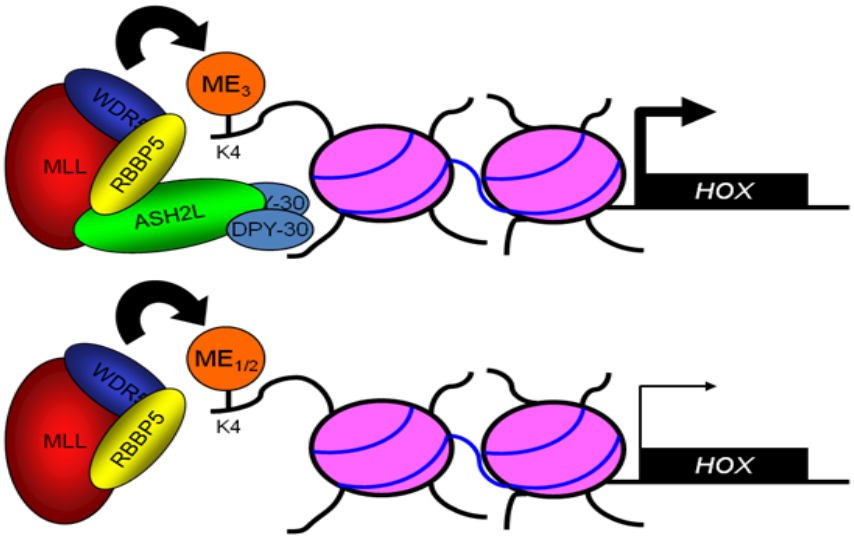

Figure 1.3 – Role of ASH2L on H3K4me3 and HOX gene expression. ASH2L when complexed with Mixed Lineage Leukemia (MLL), WDR5, RBBP5, and DPY-30 increases H3K4me3 levels and HOX gene expression during development (South and Briggs, 2011).

From the 5’ to 3’ end of the ASH2L gene, it contains a plant homeodomain (PHD) finger, a wing helix domain, a SPIa/RYanodine receptor (SPRY) domain, and a DPY-30 binding-Motif [120, 121]. The wing helix domain is associated with binding of ASH2L to the DNA and when this region is disrupted, it reduces the localization of ASH2L within the HOX locus. The SPRY domain on the C-terminal end of the ASH2L gene works with RBBP5 to regulate the methyltransferase activity of the Trithorax group of proteins [122]. For gene studies, it would be necessary to target these regions of the gene in order to have a disruptive phenotype.

Previous work in mice has shown that suppression of ASH2L globally decreases H3K4 trimethylation levels [115]. ASH2L-null mice have a lethal phenotype at embryonic Day 3.5 to 8.5 [123]. ASH2L-null embryos achieved the blastocyst stage but were non-viable in mid-gestation. Furthermore, ASH2L-null embryos were unable to establish embryonic stem cell lines. Depletion of ASH2L in mouse embryonic stem cells, led to a loss of pluripotency and a repressed transcriptional status [124]. Additionally, over expression of ASH2L is related to tumorigenesis and diseases in adults [125, 126]. Regulation of this gene in the early embryo is important due to the detrimental side effects caused by both over and under expression of ASH2L. ASH2L is also important in stabilizing X chromosome inactivation when paired with Saf-A [127]. The effect of the ASH2L on imprinted genes has yet to be analyzed. ASH2L has not been studied in mammalian models other than mice.

Research Goal and Hypothesis

Given the importance of ARTs in both human medicine and livestock industry, in vitro production of high quality, epigenetically normal embryos is essential. Further

investigation of the epigenetic modifiers during the critical period of preimplantation development is necessary to develop production systems capable of achieving this endpoint. The overall goal of this research is to characterize the role of ASH2L during early bovine preimplantation development. Our initial hypothesis was depletion or deletion of ASH2L would alter embryonic development during the preimplantation period. It was also suspected that suppression of ASH2L in the early embryo would cause variations in histone modifications and result with an altered transcriptional status. We utilized experimental techniques to examine embryonic development when ASH2L is depleted or deleted in the early bovine embryo.

We investigated the suppression or knockout of ASH2L in the early embryo by microinjection of siRNAs or CRISPR-Cas9 complexes into bovine zygotes. *In vitro* produced blastocysts depleted of ASH2L were evaluated in comparison with controls for epigenetic modifications by immunocytochemistry (ICC). ASH2L suppressed embryos and appropriate controls were transferred into recipient females and collected on Day 17 to better characterize preimplantation development. On Day 17 of development, global transcriptome analysis was performed by RNA-seq to examine if alterations were present in ASH2L embryos targeted with RNA interference. The data collected from these experiments have helped to define the role of ASH2L during preimplantation development and give insight on possible factors that can inhibit bovine IVP systems.

CHAPTER II

MATERIALS AND METHODS

RNA Interference Targeting ASH2L in Bovine Cells

Stealth siRNAs (Invitrogen) targeting the bovine ASH2L gene were tested in Madin-Darby bovine kidney (MDBK) cells. Three siRNA sequences were designed to target the sense and antisense strand of the bovine ASH2L mRNA (NM_001205473.1): ASH2L siRNA 349 (5' –GGUAGAGCUGCAGUGUGGAAUAUGU- 3'), ASH2L siRNA 1124 (5' – GAUCUCUACAGAGCCUGCUUAUAUG- 3') and ASH2L siRNA1492 (5' – CGAAGAUACAGAGACAGCCAAGUCA- 3'). Sequences shown correspond to the sense strand, with numbers indicating the target positions of the bovine ASH2L transcript. Stealth siRNAs were resuspended in nuclease-free water at a 20 μM concentration and aliquoted to avoid repeat freeze/thaw cycles. Individual or combined siRNAs were diluted to 20 nM and transfected into MDBK cells using Lipofectimin 2000 (Invitrogen). Control MDBK cells were transfected with a non-targeting siRNA (CY3, Invitrogen). RNA was extracted from transfected cells with a RNeasy kit (Qiagen) by following manufacturer guidelines. RNA was converted to cDNA and ASH2L expression ascertained by quantitative PCR (qPCR). When ASH2L targeted cells were compared to the CY3 control cells, the siRNAs of 349 and 1124 were shown to be the most effective at supressing ASH2L (Figure 2.1). An even mixture of the dual Stealth siRNAs were subsequently used for all experiments targeting the depletion of ASH2L in the embryo.

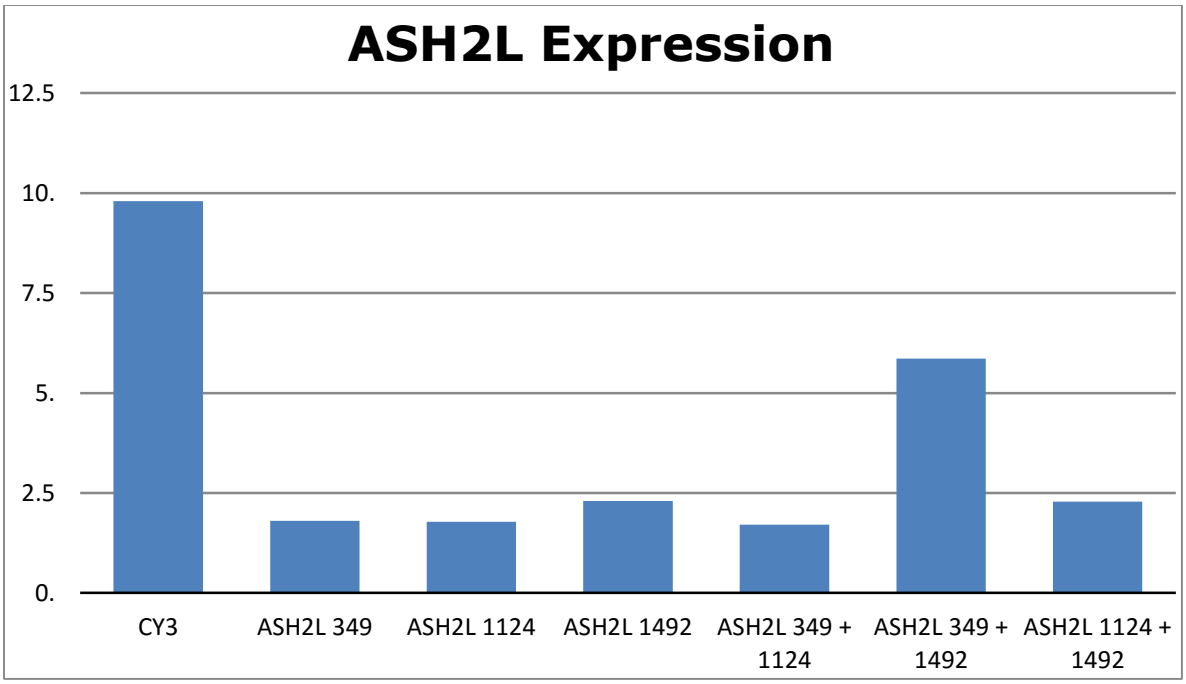

Figure 2.1 – ASH2L expression levels in cell lines transfected with siRNAs. The suppression of ASH2L is observed when compared to the control group (CY3) in Madin-Darby bovine kidney (MDBK) cells (Courtesy of Mike Peoples).

CRISPR-Cas9

Plasmid Design and Linearization

The plasmid pSpCas9 (BB)-2A-Puro (PX459) from Addgene was used for all CRISPR-Cas9 experiments for targeting the ASH2L gene (Figure 2.2). PX459 was developed by the Zheng lab (MIT) and is a modified version of the PX330 CRISPR plasmid. PX459 contains two expression cassettes that include the hSpCas9 (Cas9) and the small guide RNA (sgRNA). The chimeric backbone of the plasmid has a tracrRNA (85 nucleotides) sequence downstream of the Bbs1 cut site that allows for increased efficiency of the sgRNA. PX459 also contains the selection markers of a puromycin (Puro) and ampicillin (Amp).

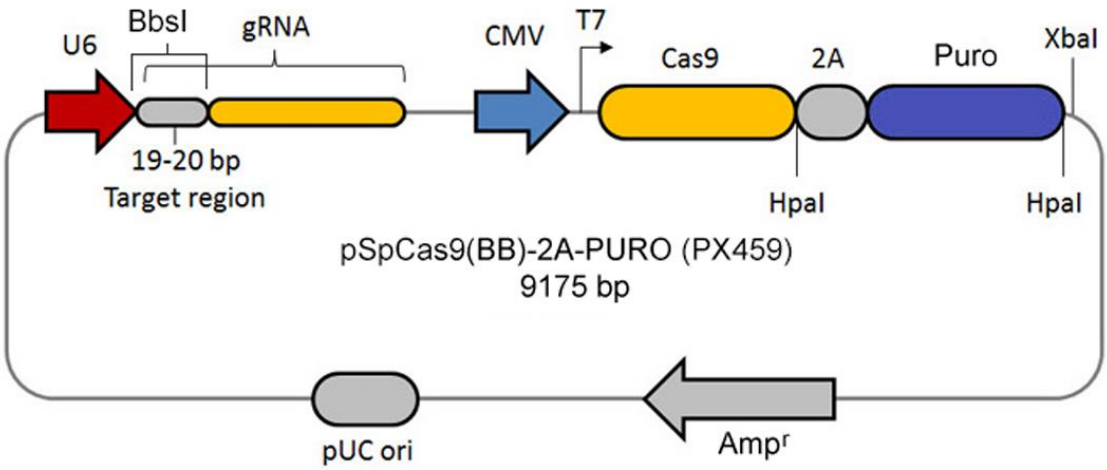

Figure 2.2 – Design of the PX459-Puro plasmid. PX459-Puro was used for insertion of guide RNA (also known as sgRNA) for future experiments targeting ASH2L gene with CRISPR-Cas9 (Courtesy of Carlos Pinzon).

Linearization of the PX459 (1 µg) was performed with a restriction digest by the following conditions: 5 µl Buffer 2.1 (NEB), 1 µl Bbs1 (NEB) enzyme, and brought up to 50 µl volume with nuclease-free water. The reaction was mixed well and digested at 37ºC for one hour and then heat inactivated at 65ºC for 20 minutes. The linearized plasmid was stored at -20ºC.

Small Guide RNA Design

The bovine ASH2L coding sequence was retrieved from the NCBI (NM_00120547) database. Each intron-exon junctions and PAM sequences (3'-NGG) were identified within the ASH2L mRNA coding sequence. Small guide RNAs were identified and then examined for off-targeting effects with NCBI Blast. After sgRNAs were verified to target the ASH2L gene and had no off-targeting effects, oligonucleotides (Invitrogen) were ordered for both the sense and antisense strand (Table 2.1). Additional nucleotides for the Bbs1 cut sites were

added to the sense and antisense strand for insertion into previously linearized plasmid (Figure A1). Oligonucleotides (Invitrogen) were resuspended in nuclease-free water at a 100 µM concentration and stored at -20ºC.

Target	Location	Strand	Oligonucleotide Sequences	PAM Sequence
ASH2L Guide 1	100	Sense	CACCGAGAAGAAGGGGAGACGAAGC	AGG
		Antisense	AAACGCTTCGTCTCCCCTTCTTCTC	
ASH2L Guide 2	49	Sense	AAACGGCCCCGGCAGCAGCTGCTAAC	
		Antisense	CACCGTTAGCAGCTGCTGCCGGGCC	TGG
ASH2L Guide 3	1422	Sense	CACCGAAACACTACTCTTCTGGCTA	CGG
		Antisense	AAACTAGCCAGAAGAGTAGTGTTTC	
ASH2L Guide 4	1439	Sense	CACCGCTACGGACAGGGAGACGTCC	TGG
		Antisense	AAACGGACGTCTCCCTGTCCGTAGC	

Table 2.1 – Oligonucleotide sequences designed for targeting ASH2L coding sequence with Bbs1 insertion nucleotides. Target sequences are underlined for each of the individual sgRNAs with PAM sequences located on the target allele. Numbers indicate the target location in the ASH2L coding sequence.

Primer Design

Primers were designed to amplify the ASH2L target sites for CRISPR-Cas9 experiments. The ASH2L sequence was retrieved from NCBI (NM_00120547) and NetPrimer (Premier Biosoft) were used to design primers for amplification of target sequences of the sgRNAs (350-600 bp). The forward and reverse primer were located at a

minimum of 100 bp away sgRNA target sequences (Table 2.2). The following conditions were used for selection of PCR primers: 20-22 nucleotides in length, Tm of 57-60˚C, GC content of 40-60%, and minimal dimerization. Oligonucleotides were reconstituted from lyophilized pellets with nuclease-free water at a concentration of 100 µM.

Target	Strand	Primers	Annealing Temperature	Amplicon Length
ASH2L Target 1	Forward	CTTTACTGTTTGAAGGTGAGCAG	60ºC	386
	Reverse	TAGGTTCGGAGGAGGGATG		
ASH2L Target 2	Forward	TGGATTTTGTGGGCATAATG	57ºC	573
	Reverse	CTAGGTATTGGGCATTTGGAC		

Table 2.2 – Primers sequences for DNA amplification of ASH2L target sites.

Insertion of sgRNA into CRISPR Plasmid

Oligonucleotides were phosphorylated individually with the following components: 2 µl of oligonucleotide stock (100 µM, Invitrogen), 2 µl of 10X T4 DNA ligase buffer (NEB), 2 µl of T4 PNK (NEB), and brought to a 20 µl volume with nuclease-free water. The reaction was mixed well and then incubated at 37˚C for 1 hour. T4 PNK was then heat inactivated at 65˚C for 20 minutes. Phosphorylated oligonucleotides were combined, 5 µl of sense and antisense, with 90 µl of nuclease-free water. The mixture was incubated for 3 minutes at 95˚C and then the reaction was slowly cooled to room temperature for one hour. To ligate the plasmid, 1 µl of annealed oligonucleotides was combined with 1.5 µl of linearized PX459, 5 µl of Rapid DNA Ligation Buffer (Rosche), 1 µl of Rapid DNA Ligation (Rosche), and

brought to a 10 µl volume with nuclease-free water. The reaction was mixed well and incubated at room temperature for 10 minutes.

After the reaction, 5 µl of the ligated mixture was added to 25 µl of TOP10 competant cells (Invitrogen) and was placed on ice for twenty minutes. The mixture was then heat shocked for 60 seconds at 42˚C to start transformation of the bacteria. After heat shock, the mixture was left on ice for two minutes to finalize the transformation. To maximize transformation efficiency, 200 µl of room temperature S.O.C Medium (Invitrogen) was then added to transformed bacteria and subsequently shaken for 1 hour at 37˚C. From the mixture, 150 µl was pipetted onto a prewarmed LB agar-ampicillin plate and placed in a 37˚C incubator for 12-16 hours. Plates were then examined for colony formation and moved to 4˚C for storage.

Individual colonies were selected and placed into tubes with 2 ml of LB Broth (Invitrogen) supplemented with 1 µg/ml of Ampicillin. Tubes were shaken overnight at 37˚C to propagate the bacteria. After propagation, bacterial DNA was then isolated from the LB Broth with Qiagen Miniprep Kit (Qiagen). DNA was examined for concentration, purity (NanoDrop, Thermo Scientific), and then stored at -20˚C.

Verification of sgRNA Insertion into Plasmid

Purified DNA (1 µg) from the transformed plasmids underwent a restriction digest to determine if the guide sequence was inserted into PX459. DNA was double digested with 0.5 µl Ecor1 (NEB), 0.5 µl Bbs1 (NEB), 2 µl Buffer 2.1 (NEB), and adjusted the volume to 20 µl with nuclease-free water. A positive control of untransformed PX459 and negative control with water were substituted for the transformed plasmid. The mixture was digested for 1 hour

at 37˚C in a humidified incubator and then heat inactivated at 65˚C for 20 minutes. The reaction was then analyzed on a 1% agarose gel to see if the Bbs1 site was destroyed from the insertion of the sgRNA (Figure A2).

Transfection of CRISPR-Cas9 Complex into Bovine Cells

Culture of Bovine Fibroblast Cells

Early passage bovine fibroblast cells, produced at the Reproductive Science Lab (Bryan, TX), were maintained in T75 tissue culture flasks (VWR) and cultured in an incubator at 37˚C, 5% CO_2, and humidified air. Cells were cultured in Dulbecco's Modified Eagle Medium with nutrient mixture F-12 (DMEM/F12, Life Technologies) supplemented with 10% fetal bovine serum (FBS, Atlanta Biologicals), 1% antibiotic/antimycotic (Anti-Anti, Life Technologies), and 50mg/ml gentamicin (Life Technologies). Cells were passed once they obtained a confluency of 80-90% in order to maintain cell viability. During the passage of fibroblast cells, the cells were washed twice with 10 ml of calcium and magnesium free DPBS (Life Technologies) and then 2 ml of trypsin (Trypsin-EDTA 0.25%, Life Technologies) was added onto to the cells. The cells incubated in the trypsin at 37˚C until the cells released from the bottom of the flask. Once the cells were released, the trypsin was neutralized with 10% culture media (DMEM/F12, 10% FBS, 1% antibiotic-antimycotic (Gibco), and 50 mg/ml gentamicin), and centrifuged for 5 minutes at 200x g. The supernatant, with the trypsin, was removed and replaced with prewarmed culture media and divided evenly amongst new culture flasks. For transfections, fibroblast cells were plated eighteen hours pretransfection into a 6-well polystyrene culture dish (VWR) so monolayer of cells reached 70-80% confluency at the time of the transfection.

Preparation of PolyJet-DNA Complex for Transfection

Plasmid DNA (1 µg), with inserted sgRNA, was diluted in 50 µl of DMEM with high glucose (Gibco) in a 0.6 ml conical tube. In a separate 0.6 ml conical tube, 3 µl of PolyJet (SignaGen Laboratories) was diluted in 50 µl of DMEM with high glucose. Once mixed, the diluted PolyJet was added to plasmid DNA and incubated for 12 minutes at room temperature to allow the PolyJet/DNA complex to form. After incubation, the PolyJet/DNA complex was evenly added drop by drop to bovine fibroblast cells and incubated at 37˚C for 12 hours. Fresh 10% culture media (2 ml) was then added to each group of cells. For each transfection, the plasmid PX458-GFP (Addgene, Plasmid #48138) was added to a separate group of cells to serve as a positive control and allowed visual determination of transfection efficiency (Figure A4).

Puromycin Selection and Single Cell Colony Propagation

After transfections, bovine fibroblast cells were allowed to recover for 36 hours in 10% culture media before selection of positive colonies with puromycin (Invitrogen). Puromycin, at a concentration of 1 µg/ml, was added to 10% culture media for 72 hours or until single cell colonies were visible. Singe cell colonies then recuperated in 20% culture media (DMEM/F12, 20% FBS, 1%Anti-Anti, and 50mg/ml Gentamicin) for 24 hours. Clonal rings (Scienceware) was then used for selection of single cell colonies. Trypsin was added drop by drop until it covered the cell and was incubated at 37˚C for 5 minutes or until the cell released from the well. The 20% culture media was added to clonal ring to collect cell and was transferred to a 24-well polystyrene plate (VWR) to continue culture.

DNA Extraction and Preparation for Sequencing

DNA Extraction from Bovine Cells

A DNeasy kit (Qiagen) was used to isolate DNA from the proliferated single cell colonies. DNA extraction was performed according to manufacturer guidelines except 30 µl of elution buffer was used to increase DNA concentration. DNA was examined for concentration, purity (NanoDrop, Thermo Scientific), and stored at -20˚C or amplified immediately by PCR.

DNA Extraction from Embryos

On Day 8 post IVF, blastocysts from sgASH2L Target 1 and Target 2 groups were washed twice through DPBS to rinse any culture media and mineral oil away. Embryos were then exposed to Tyrode's Salt Acidic (TSA, Invitrogen) for 2 to 5 minutes or until the zona pellucida was removed. The embryo was then washed three more times in DPBS and placed into 10 µl of lysis buffer (Buffer AL, Qiagen) with a sterile Drummond pipet. A new pipet was used for each embryo to avoid cross contamination of the DNA. Embryos were then stored at -20ºC until DNA extraction.

Embryos were thawed and 50 µl of lysis buffer was added to each sample. Lysed embryos were exposed to EDTA, Tris·HCl, and Proteinase K (Qiagen); and incubated at 45ºC for 1 hour to digest any proteins. After incubation, a 1:1 ratio of phenol chloroform: isoamyl alcohol (Sigma) was added to each embryo sample. Embryos were vortexed and centrifuged at 13,000x g for 10 minutes at room temperature. The aqueous layer (top layer) was transferred to a sterile 0.6 mL conical tube (VWR). Double the volume of 100% ethanol was added to precipitate the DNA and was stored overnight at -20ºC. Precipitated DNA was

pelleted by centrifugation at 13,000x g for 30 minutes at 4ºC. Ethanol was then removed from the pelleted DNA and washed again with freshly prepared 70% ethanol at 13,000x g for 10 minutes at 4ºC. Ethanol was removed from the pellet and was air dried for 5 to 10 minutes. The dried pellet was resuspended in 10 µl of filtered TE Buffer and stored at -20ºC.

DNA Amplification for sgRNA Target Regions

DNA extracted from individual cell colonies and embryos were used for PCR amplification of target regions for the sgRNAs. A mastermix was made with the following components for each reaction: 2.5 µl 10X buffer (Invitrogen), 0.5 µl dNTPs (Promega), 0.5 µl forward primer (Target 1 or Target 2), 0.5 µl reverse primer (Target1 or Target 2), 0.75 µl $MgCl_2$ (Invitrogen), 0.125 µl taq polymerase (Invitrogen), and brought to a 21 µl volume with nuclease-free water (Table A1). The master mix was vortexed, centrifuged down, and aliquoted into individual PCR tubes. DNA from the individual embryo or cell colony (4 µl) was added to the mastermix, vortexed, and then centrifuged down. For each reaction, a positive bovine genomic DNA and negative water control were used. The reactions were placed into the thermo cycler (Peltier) and exposed to the respective conditions for sgASH2L Target 1 or Target 2 (Table A2 and Table A3, respectively). Once the reaction was complete, the samples were stored at -20ºC or went directly for gel analysis.

DNA from the PCR reaction was mixed with a 1:6 dilution of loading dye (Invitrogen) and was visually analyzed by 1% agarose (Invitrogen) gel, with GelRed (Phenix) being used as a nucleic acid stain. The 1kb+ ladder (Invitrogen) was used to reference of the size (Target 1- 386 bp or Target 2- 573 bp) of the amplified DNA. After positive lanes were identified, an additional PCR reaction was made as previoiusly described

for DNA from the individual embryos (Table A1). Positive DNA bands were stabbed from the gel with a 20 µl pipet tip and placed into the PCR premix. The DNA underwent an additional amplification in order to increase the total amount of DNA obtained from individual embryos. After the DNA was amplified, it was gel analyzed under the same conditions previously described. Once a positive lane was identified, the remaining 15 µl of amplified DNA was extracted with a PCR Purification Kit (Invitrogen). DNA purification was completed by following manufacturer guidelines with a change in the elution step. DNA was eluted with 25 µl of prewarmed nuclease-free water in order to increase DNA concentration from the colomn. DNA was then stored at -20ºC or was used for sequence analysis.

Sequence Analysis

DNA was examined for concentration and quality before being sent for sequence analysis. DNA was sequenced with an ABI PRISM(R) 3100 Genetic Analyzer at the Gene Technology Laboratory (GTL) on the Texas A&M campus. Plasmid DNA was sent for sequencing at a concentration of 400-600 ng/µl while DNA from PCR purification was sent at a concentration of 10ng/100bp. All sequence primers were sent in at a concentration of 6-10 pM per sequence reaction. The Primer LKO 1.5'- GACTATCATATGCTTACCGT was used to sequence the PX459 plasmid for insertion of the sgRNAs (Figure A5). DNA from single-cell colonies and individual embryos were sequenced with the forward primer for each of the respective target regions. Sequences were retrieved from the GTL website and sequence analysis was completed with NCBI Blast to analyze sequence result with the wild type sequence. Chromatographs from the sequences were analyzed with ApE software to

examine if mutations present were suggested to be monoallelic (Figure A6) or biallelic (Figure A7).

Bovine Embryo Production

In Vitro Embryo Production and Culture

Bovine oocytes were collected from a commercial vendor (DeSoto Biosciences, Seymour, TN) and shipped in an MOFA metal bead incubator (MOFA Global) overnight at 38.5˚C in sealed vials containing 5% CO_2 in air-equilibrated Medium 199 with Earle's salts (Gibco), 10% fetal bovine serum (Hyclone), 1% penicillin–streptomycin (Invitrogen), 0.2-mM sodium pyruvate, 2-mM L-glutamine (Sigma), and 5.0 mg/mL of Folltropin (Vetoquinol). Only high quality oocytes were selected for embryo experiments. Once oocytes were matured (22-24 hours), they were washed twice in warm Tyrode lactate (TL) HEPES (MOFA) media supplemented with 50 mg/ml of gentamicin (Invitrogen) while being handled on a 38.5˚C stage warmer. Fertilization stock medium contained the following ingredients: 114 mM NaCl (Sigma), 3.2 mM KCl (Sigma), 25.0 mM $NaHCO_3$ (Sigma), 0.34 mM NaH_2PO_4•H2O (Sigma), 10 mM Na Lactate (Sigma), 1µl/ml Phenol Red (Sigma), 2.0 mM $CaCl_2$.2H20 (Sigma), and 0.5 mM $MgCl_2$.6H20 (Sigma). Fertilization stock medium was supplemented the day of IVF with 250-mM sodium pyruvate (Sigma), 1% penicillin–streptomycin (Gibco), 6 mg/mL of fatty acid–free BSA (Sigma), 20-mM penicillamine (Sigma), 10-mM hypotaurine (Sigma), and 10 mg/mL of heparin (Sigma). The fertilization medium was pre-equilibrated at 38.5˚C in a 5% CO_2 humidified air incubator for at least 2 hours before the start of IVF procedures. Oocytes were washed once in bovine fertilization media and then was placed into the fertization well. Frozen semen (Logan 62M27,

Beefmaster, Lot 03237) was thawed at 35˚C for 1 minute, then live/dead separated by centrifugation at 200x g for 20 minutes in a density gradient medium (Isolate, Irvine Scientific). The supernatant was removed and 200 µl of sperm pellet was resuspended in 2 ml of pre-equilibated bovine fertilization media and centrifuged at 200x g for 10 minutes. The sperm pellet was removed and placed into a warm 0.65-ml microtube (VWR). A 1:20 dilution of the semen pellet in ddH20 was placed onto a hemocytometer with averages the two counts being used to calculate sperm concentration. Semen was diluted in pre-equilibrated fertilization media before bulk fertilization in Nunclon four-well dishes (VWR) containing up to 50 matured oocytes per well at a concentration of 1.0 x 10^6 sperm/ml. Embryo development for the transfers were preformed with the some modifications. The sire was a *bos indicus* bull (Suville Poncrata 102, Brahman, Lot 89387) and the following modifications were made to bovine fertilization media to optimize fertilization conditions for the sire: 20 µg/ml heparin, 2.0 x 10^6 sperm/ml, and fertilization occurred in 50 µl drops.

Fertilization lasted for 16 to 18 hours in a 5% CO_2 and humidified air incubator. Presumptive zygotes were washed out of fertilization media and placed into TL Hepes. The cumulus cells were removed by a 2-minute vortex in 45 µl of TL HEPES in a 0.65 ml microtube (VWR). Cumulus cells not removed by vortex were cleaned with a 125 µM stripper tip (Origio). Presumptive zygotes underwent multiple washes to be separated from cumulous cells. Once presumptive zygotes were cleaned, they were placed into Bovine Evolve medium (Zenith Biotech) supplemented with 4 mg/ml of BSA (Probumin, Millipore). Embryos were cultured in groups of approximately one embryo per 10 µl of culture media (50 embryos/500µl Bovine Evolve) in a 5% CO_2 and 5% O_2 humidified incubator. Cleavage rates were recorded on Day 2, and viable embryos were separated from nonviable embryos at

this time. Embryos were monitored daily for morphologic progression, and blastocyst rates were recorded on Day 8 post IVF.

Cas9 mRNA and sgRNA Preparation for Microinjections

In Vitro Transcription of Cas9 mRNA

The linearized PX459 plasmid was used for production of the Cas9 messenger RNA (mRNA). Production of the Cas9 mRNA was prepared by *in vitro* transcription (IVT) with the T7 mMESSAGE mMACHINE Kit (Ambion), with 1 µg of DNA template being used. IVT, extraction, and purification of the Cas9 mRNA was prepared by following manufacturer guidelines. Cas9 mRNA was resuspended in TE Buffer and analyzed for concentration and purity. Cas9 mRNA was then aliquoted into 0.65 ml microtubes to avoid repeated freeze/thaw cycles and stored at -80˚C.

Production of sgRNAs for Microinjections

Plasmids verified for the insertion of the target sequence for ASH2L were used for the production of sgRNAs. PX459 does not have a T7 promoter located upstream of the sgRNA sequence so a forward primer was designed with a T7 promoter on the 5’ end of the Bbs1 insertion region and reverse primer on the 3’ end of the tracrRNA sequence (Figure A8). This allows for insertion of the promoter sequence and amplification of the sgRNA sequence needed for *in vitro* transcription (IVT).

The PCR reaction was mixed under the following conditions: 12.5 µl of Hifi PCR Premix (CloneAmp), 0.5 µl forward primer, 0.5 µl reverse primer, 100 ng of DNA template, and brought to a 25 µl volume with nuclease-free water. The T7 promoter and target

sequence was then PCR amplified in a thermo cycler under the appropriate conditions (Table A4). The DNA from the PCR was then placed on a 1% agarose gel to analyze amplification of the target sequence with the T7 promoter. After visual confirmation, a QIAquick Gel Extraction Kit (Qiagen) was used for extracting the T7 promoter and target sequence. After the DNA was eluted, it was analyzed for concentration and quality and then stored at -20˚C until future use.

After insertion of the T7 promoter upstream of the sgRNA sequence and extraction of plasmid DNA, each of the plasmids were *in vitro* transcribed with the T7 MEGASCRIPT Kit (Ambion) in order to produce the sgRNAs. IVT was completed by following manufacturer guidelines with a 4 hour incubation time for the reaction. After terminating the reaction, the sgRNA was collected with a phenol:chloroform extraction and isopropanol precipitation. The sgRNA was resuspended in TE Buffer and analyzed for concentration and purity. The sgRNAs were aliquoted into 0.65 ml microtubes and stored at -80˚C.

Bovine Intracytoplasmic Microinjections

Microinjections of siRNAs Targeting ASH2L

Presumptive zygotes were randomly assigned to three different treatment groups: non-injected controls (Control), non-targeting siRNA injected controls (siNULL), and injection with dual siRNAs targeting ASH2L (siASH2L). The siNULL embryos were injected with a fluorescently (Cy3) labeled negative control siRNA (Invitrogen) mixed with a green fluorescent dextran (Invitrogen) in TE buffer. The siASH2L embryos were injected with target verified siRNAs (20 nM), and mixed with a green fluorescent dextran in TE buffer. The green fluorescent dextran was used for visual confirmation of the

intracytoplasmic microinjections (Figure 2.3). Presumptive zygotes from the siNULL and siASH2L groups were injected with approximately 100 pl of there respective construct. After injection, fluorescent embryos were placed back into Bovine Evolve medium (Zenith Biotech) and cultured in a humidified incubator with the gas concentrations of 5% CO_2, 5% O_2, and 90% N_2.

Figure 2.3 – Representative image of intracytoplasmic microinjection in bovine embryos. Microcinjections of siRNAs targeting ASH2L or CRISPR-Cas9 complex targeting ASH2L into presumptive bovine zygote (A) with confirmation of microinjection taking place (B) (Courtesy of Jane Pryor).

Microinjections of CRISPR-Cas9 Complex Targeting ASH2L

Presumptive zygotes were randomly assigned to four different treatment groups: non-injected controls (Control), sham-injected controls (sgNULL), sgASH2L Target 1 (Guide 1 and Guide 2), and sgASH2L Target 2 (Guide 3 and Guide 4). Prior to microinjections, Cas9 mRNA and the dual sgRNAs were mixed and incubated on ice for 20 minutes to create the CRISPR-Cas9 target cascade. The non-targeting injection controls were made with the dual sgRNAs (25 ng/µl each), a green fluorescent dextran, and mixed in TE Buffer. Each sgASH2L target group was mixed with Cas9 mRNA (40 ng/µl), the respective dual sgRNAs

(25 ng/µl), green fluorescent dextran, and suspended in TE Buffer. Presumptive zygotes were injected with approximately 100 pl with their respective construct (Figure 2.3). After injection, fluorescent embryos were placed into Bovine Evolve medium (Zenith Biotech) and cultured in a humidified incubator with the gas concentrations of 5% CO_2, 5% O_2, and 90% N_2.

Expression Levels of ASH2L in Suppressed Embryos

RNA Extraction and Reverse Transcription

RNA was extracted from 3 biological repititions of each treatment group at the 8-cell (N=15) and blastocyst (N=10) stage of development by using RNeasy Mini Kit (Qiagen). RNA was extracted by following manufacturer protocol with one modification. Due to the lower concentration of RNA present in these samples, each was eluted with 20 µl of nuclease-free water. RNA was DNase treated by adding 1 µl of DNase Buffer (Invitrogen), 1 µl DNase (Invitrogen), and incubated at 65ºC for 10 minutes. Reverse transcription reactions were performed by using the SuperScriptII kit (Invitrogen) by combining 1 µl of 10mM dNTP (Promega), 1 µl of random hexamer oligonucleotides (Invitrogen), 8.5 µl of nuclease-free water, and 2.5 µl of DNase treated RNA. The constant volume was done due to the low concentration of RNA from the embryos that is unable to be detected (NanoDrop, Thermo Scientific). The DNase treated RNA was separated into four groups for reverse transcription with one sample of being used to create a negative control for the qPCR step and did not undergo reverse transcription. The reaction ran for 5 minutes at 70°C and then cooled to room temperature. Volumes of 5 µl of SuperScriptII (Invitrogen) reaction buffer, 3 µl dithiothreitol (Invitrogen), and 1 µl SuperScriptII (Invitrogen) were then added to the

reaction mixture. The mixture was then incubated for 50 minutes at 42°C, 20 minutes at 45°C, 15 minutes at 50°C, and then 5 minutes at 70°C. After the incubation, the cDNA samples were stored at -20°C or went directly to quantitative PCR.

Quantitative PCR

Quantitative PCR (qPCR) analysis of the cDNA was performed by using 6.25 µl of DyNAmo Flash SYBR Green qPCR Mastermix (Fisher Scientific), 0.25 µl Forward and Reverse Primer (125pM), 0.25 ROX inhibitor (Invitrogen), 5 µl cDNA (0.6 µM) or negative control and brought up to a volume of 12.5 µl with nuclease-free water. The reactions were loaded into a 96 well plate with the reactions being performed with a StepOnePlus Real-Time PCR system (Applied Biosystems). Relative gene expression levels from each sample was calculated in triplicate by using the SYBR Green comparative ΔC_t method.

Immunocytochemistry

Fixing of Bovine Blastocyst Embryos

For each treatment group (N=12), a minimum of 3 biological repitions of blastocyst stage embryos was removed from culture media, washed twice with DPBS (Life Technologies), and fixed with ice-cold 99% methanol for a minimum of one minute. Embryos were washed in DPBS with 0.1% Tween-20 (Sigma, 0.1% DPBS-Tween) and stored at 4˚C until future use.

Labelling for 5mc, 5hmc, and Posttranslational Histone Modifications

Fixed blastocyst embryos were permeabilized for 15 minutes at room temperature with 1% Triton X-100, diluted in DPBS, and then washed 3 times for 5 minutes each in 0.1% DPBS-Tween. Embryos used for examination of cytosine methylation and hydroxymethylation were treated with 2M HCl diluted in ddH_2O, for removal of the zona pellucida. The embryos were removed from the 2M HCl once the zona pellucida was dissolved (10-15 minutes). The embryos were washed through 100 mM Trizma hydrochloride buffer (pH 8.5) for 10 minutes at room temperature to neutralize the HCl. All embryo groups were washed through 0.1% DPBS-Tween and then incubated in blocking buffer (10 mg/mL of BSA, 2% goat serum, and 11.25 mg/mL of glycine in DPBS) overnight at 4˚C. Embryos were then placed into 500 µl of diluted (1:200) primary antibodies (Table 2.4) in blocking buffer for 1 hour at room temperature. Negative control embryos were incubated in blocking buffer with no primary antibody present. Embryos were washed through blocking buffer 3 times for 30 minutes each. Alexa 488 (Invitrogen) and Alexa 594 (Invitrogen) were diluted (1:200) in 0.1% DPBS-Tween and embryos were incubated for 1 hour at room temperature with no light. The remaining steps were carried out with no light. The secondary antibody labeled embryos were washed 3 times for 30 minutes each in 0.1% DPBS-Tw. Hoechst (Sigma) was diluted at a concentration of 5 µg/ml in DPBS and embryos were added for 15 minutes at room temperature. Embryos were washed three times with 0.1% DPBS-Tw for 5 minutes each at room temperature. Embryos were placed in a 20 µl mounting media 50-50 solution of antifade and glycerol with a diluted 5 µg/ml of Hoechst. Cover slips were mounted with parafilm wax on the edge to prevent damage of the embryos and sealed with clear fingernail polish for storage at -20ºC.

Type	Target	Antibody	Source (cat#)
Primary	5mc	5-Methylcytidine mAb	Epigentek (33D3)
Primary	5hmc	5-Hydroxymethylcytosine pAb	Active Motif (39791)
Primary	H3K4me3	Histone 3 trimethyl Lys4 Rabbit pAb	Active Motif (39159)
Primary	H3K4me2	Histone 3 dimethyl Lys4 Rabbit pAb	Abcam (ab11946)
Primary	H3K9me2-3	Histone 3 di-trimethyl Lys9 Rabbit mAb	Abcam (ab71604)
Primary	H3K27me3	Histone 3 trimethyl Lys27 Rabbit mAb	Abcam (ab6002)
Secondary	Rabbit IgG	Alexa Flour 488 Goat Anti-Rabbit IgG	Invitrogen (A-11008)
Secondary	Goat IgG	Alexa Flour 488 Donkey Anti-Goat IgG	Invitrogen (A-11055)
Secondary	Mouse IgG	Alexa Flour 594 Goat Anti-Rabbit IgG	Invitrogen (A-11005)

Table 2.3 – Primary and secondary antibodies used for ICC.

Digital Microscopy and Analysis

Digital imaging microscopy was performed at the Texas A&M University, College of Veterinary Medicine and Biomedical Sciences Image Analysis Laboratory at the Zeiss Stallion digital imaging workstation. Z-series were taken from individual embryos that were equally represented with five images taken from top to bottom of the embryo with various sizes and shapes depending on the embryo. Each photograph had an image of the DNA stain (Hoechst), image for the antibody of interest, and a merge of all images. Intensity measurements were taken using NIS Elements 3.0 (Nikon) software. Mean intensity measurements were set at a baseline level with negative control embryos that were only secondary antibody labeled. The mean flourescent intensity measurement for the targeting

antibody was divided by the DNA stained nuclei to give a fluorescent intensity ratio for each embryo.

Embryo Transfer and Collection of Day 17 Conceptuses

Estrous Synchronization of Recipient Cows

Fourteen reproductively mature cows were prepalpated and examined for reproductive soundness before being utilized for estrous synchronization. On the morning of Day -9 IVF, cycling cows were given a 2cc Combo Injection (Progesterone and Estradiol 17-beta, Med Shop 280881) and a sterilized EAZI-BREED CIDR (Pfizer S1104231) being properly placed into the cycling cow. On Day -2 IVF, the EAZI-BREED CIDR was pulled and each cow was given a 5cc injection of prostaglandin (Lutalyse, Zoetis). The following afternoon, recipient cows were given a 1cc injection of Estradiol 17-beta (Med Shop 280883) with expected synchrony to occur the following day. The synchronized recipients waited until Day 7 for siNULL and siASH2L embryos to be transferred.

Embryo Transfer of Day 7 Embryos

On Day 7 post-IVF, embryos were graded for development and quality. Blastocyst and morula staged embryos from the siNULL and siASH2L groups were washed into Vigro holding media (BioNiche) and loaded into ¼ cc straws (PETS), with two to five embryos per straw. Once the embryos were loaded, straws were placed in a 38.5ºC Micro-Q straw warmer to wait for transfer. Straws with embryos were loaded into 0.25 transfer sheaths (PETS) and transferred ipsilateral to the side of the corpus luteum (CL) with an embryo transfer gun (Dr.

Looney, Ovagenix, Bryan, TX). If no CL was present the receipt was not used for the experiment.

Day 17 Conceptus Collection and Morphological Analysis

On Day 17 post IVF, previously transferred siNULL and siASH2L embryos were collected from the cows (Dr. Looney, Ovagenix). Embryos were collected with one liter of lactated ringers supplemented with FBS, a 22 gauge BARD Foley Catheter (PETS), and collected into an EZ Way Filter (PETS). The filter was rinsed three times with 30 ml of rinsing media (BioNiche). Filters were then searched for Day 17 conceptuses within the dish and placed into 35 mm petri dish, with TL HEPES once found. Conceptuses were collected and washed five times in TL HEPES to wash the conceptus out of uterine fluid and rinsing media from the collection. Day 17 conceptuses were examined for an embryonic disc and size of the filamentous conceptus was recorded. The Day 17 conceptuses for the siNULL and siASH2L groups were washed out of TL HEPES five times in DPBS. Once the embryos were washed, they were placed in a minimal amount of DPBS and stored at -80ºC until RNA extraction.

RNA Sequencing and Pathway Validation

RNA Extraction and Sequencing

RNA extraction and genomic DNA elimination from the Day 17 conceptus was completed by using RNeasy Plus Mini kit (Qiagen). After extraction, RNA was examined for concentration, purity, and then stored at -80˚C. If RNA met quality standards (1.9-2.1) and had high enough concentration (15 ng/µl) it was sent to the Whitehead Institute

(Massachusetts Institute for Technology) for RNA prep and RNA-seq. RNA from conceptuses from siASH2L (N=4) and siNULL (N=3) embryos were sent in for RNA-seq.

Once quality was verified, RNA samples underwent library preparation and sequencing (1µg RNA in 20µl nuclease free water). Libraries were pooled for each embryo group and then sequenced on an Illumina HISEQ 2500 (pair-end, 2x100 bp). The RNA-seq reads were assessed for quality with FastQC. Adapters were removed with Cutadapt and processed for quality with FastX-toolkit.

Pathway Validation

After RNA-seq analysis, significantly altered genes from common pathways had primers designed for quantitative PCR (qPCR). Primers were designed as previously described in the methods section of Primer Design for quantification analysis of the genes in developmental pathways (Table 2.4). Conceptuses of the siNULL (N=4) and siASH2L (N=4) groups for used for analysis with duplicate reverse transcription reactions being performed. Reverse transcription was carried out with 250 ng/µl for each reaction by following the conditions as previously defined. The qPCR reaction was carried out as before described for analysis of ASH2L in 8-cell and blastocyst embryos.

Gene	Strand	Primer Sequence
ZFP3	Forward	GTAGCTGCCTGAGATTGTGAG
	Reverse	TGCTCCAAACTCATGACCCT
ZNF521	Forward	ACATGATTGATGAAGGGCTG
	Reverse	TTGGGTCATCGTATGGTTCTG
DLX5	Forward	CTACCGATTCCGACTACTACAG
	Reverse	ACTTCTTTCTCTGGCTGGCT
CCL27	Forward	GTGTGAGTCCCTGTCCCAAG
	Reverse	GTGCACACGAGGGAAGATCA
WNT11	Forward	GACACTCTGACAGTGGACAGG
	Reverse	GGAGCATCGGAAAACTTGGC
GAPDH	Forward	CTGCCCGTTCGACAGATAG
	Reverse	CTCCGACCTTCACCATCTTG
SDHA	Forward	ACCTGATGCTTTGTGCTCTG
	Reverse	TCGTACTCGTCAACCCTCTC
YWAHZ	Forward	CTGAACTCCCCTGAGAAAGC
	Reverse	CCTTCTCCTGCTTCAGCTTC

Table 2.4 – Primers used for quantitative amplification of bovine genes. Forward and reverse primers were designed for both the reference genes (GAPDH, SDHA, and YWAHZ) and genes of interest (ZFP3, ZNF521, DLX5, CCL27, and WNT11).

Statistical Analysis

Embryo Development

Statistical analysis for developmental data was performed using GraphPad Prism 6 (GraphPad Software, Inc). Cleavage and blastocyst rates underwent an arcsine square root transformation to make the distribution normal. A One-Way ANOVA was used to compare the means of the three treatment groups, alpha was set at 0.05. If significant differences were observed a Tukey HSD test was used to determine which development group was significant.

Real-time Quantitative PCR

CT values from three biological replicates were normalized to the geometric mean of the bovine reference genes (GAPDH, SDHA, and YWHAZ) [128]. Relative gene expression levels were obtained in triplicates by using the ΔΔCT method. Values obtained were then analyzed by the GraphPad Prism 6 (GraphPad Software, Inc). Data underwent log transformation to make data more symmetrical. A One-Way ANOVA was used to compare the means of the three treatment groups, alpha was set at 0.05. If significant difference was observed a Tukey HSD test was utilized to determine what treatment groups was significant. Analysis with only two treatment groups was performed with a Student t-test.

Immunocytochemistry

Statistical analysis for fluorescence intensity ratios generated by ICC was completed with the software program JMP (SAS software). Developmental data was checked for normality with a Shapiro-Wilk test with outliers within each treatment group being identified with Quantile Range Outliers. A One-Way ANOVA was used to compare the means of the three treatment groups, alpha was set at 0.05. If significant differences were observed, a Tukey HSD test was performed.

RNA Sequence

Day 17 conceptuses of similar morphological sizes were compared with each other for RNA-seq analysis. RNA expression levels were determined with Cuffmerge and Cuffdiff. Statistical analysis and visualization was performed with R, using RStudio running cummeRbund. Read depth was a minimum of ten counts per mRNA for each gene. A log

ratio of 1.5 was used to determine the threshold. Pathway analysis was examined by using Ingenuity software with a significant value set at $p<0.05$.

CHAPTER III

RESULTS

Embryo Development

RNA Interference Targeting ASH2L

After five rounds of IVF, embryos (N=1,309) were examined for cleavage and blastocysts rates between the Control, siNULL, and siASH2L groups. Analysis of embryo cleavage rates showed no significant difference between each of the treatment groups ($p=0.27$, Figure 3.1, Table 3.1). On Day 8, the Control embryos tended to have higher blastocyst rates ($p=0.06$). When siASH2L embryos were compared with siNULL, no significant difference was observed in blastocyst development (31.3% vs 33.3%, respectively $p>0.2$). All embryo groups developed to the blastocyst stage with good morphology and a low number of extruded cells, suggesting good quality embryos in each treatment group (Figure 3.2).

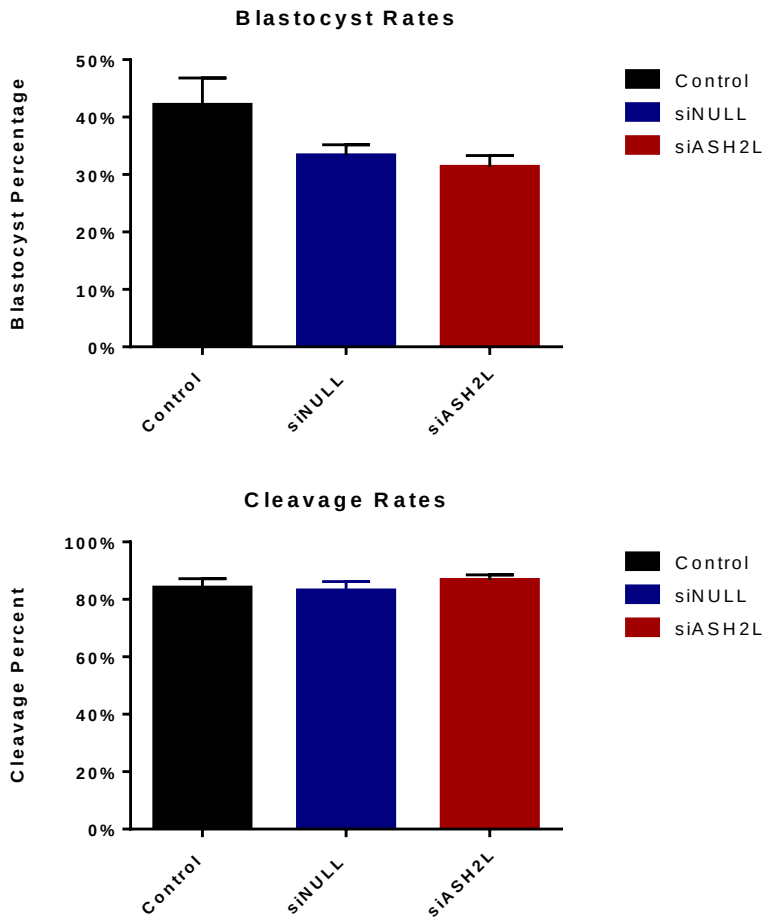

Figure 3.1- Cleavage and blastocyst rates for bovine embryos in the Control, siNULL, and siASH2L embryo groups. Data was analyzed with a one-way ANOVA and Tukey HSD, alpha was set at 0.05.

Treatment	Number Cultured	Number Cleaved	Percent Cleaved	Number Blastocyst	Percent Blastocyst
Control	425	357	84.0 ± 3.2%[a]	179	42.1 ± 4.7%[a]
siNULL	418	347	83.0 ± 4.2%[a]	139	33.3 ± 1.9%[a]
siASH2L	466	404	86.7 ± 1.8%[a]	146	31.3 ± 2.0%[a]

Table 3.1 - Embryo development rates ± S.E.M for Control, siNULL, and siASH2L embryo groups. Same letter indicates no sirnigicant difference amongst each of the embryo groups.

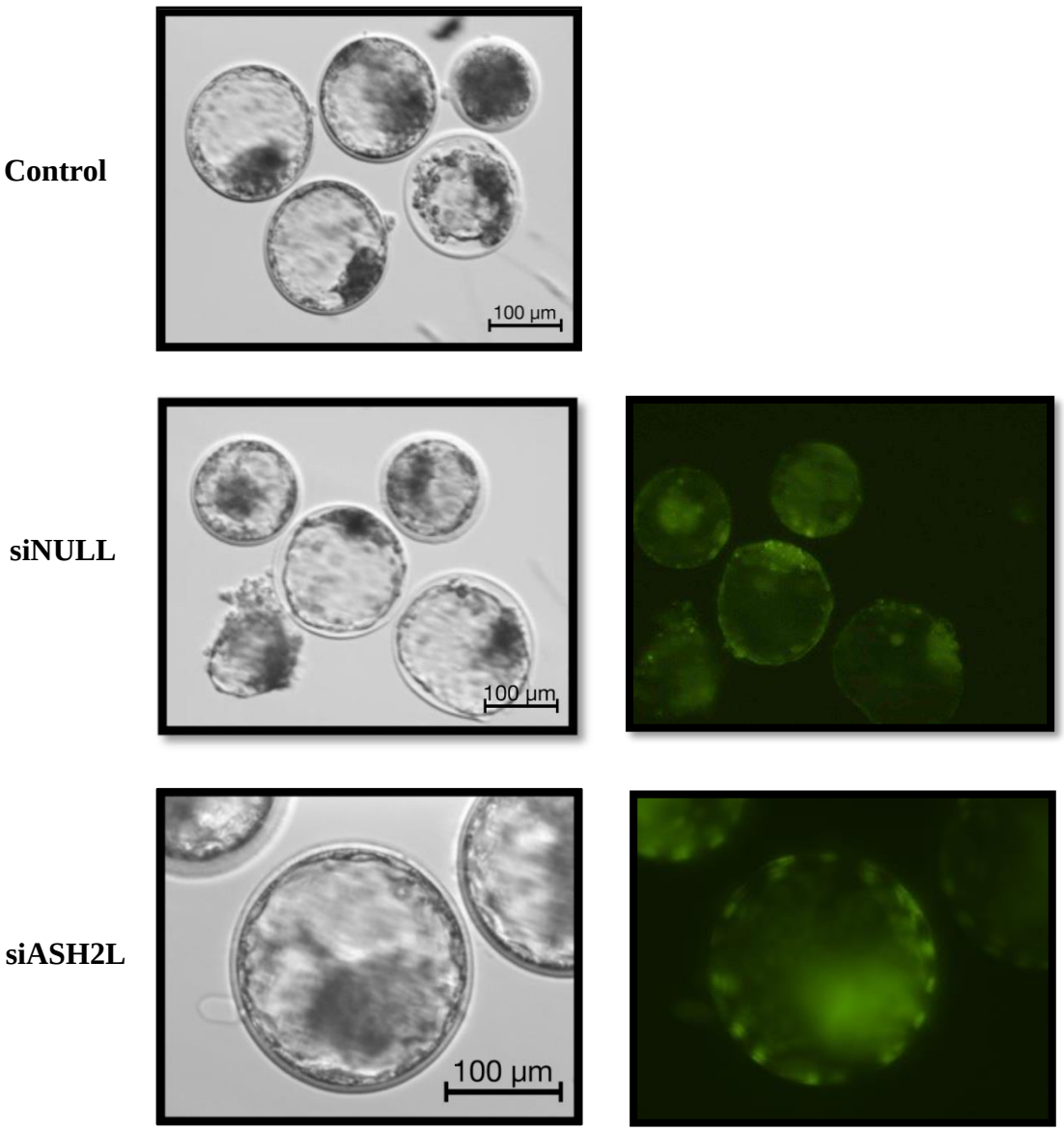

Figure 3.2 – Representative images of blastocysts embryos on Day 8 of development. Bright field images were taken for the Control (20X), siNULL (20X), and siASH2L (40X) embryos. Fluorescent photos (right image) are shown in the siNULL and siASH2L for visual confirmation of microinjection.

CRISPR-Cas9 Targeting ASH2L

After three rounds of IVF and microinjections, embryos (N=770) were analyzed for cleavage and blastocysts rates between the Control, sgNULL, sgASH2L Target 1, and sgASH2L Target 2 embyro groups. Cleavage rates were consistent between all embryo

groups (Figure 3.3, Table 3.2). Blastocysts rates for the sgNULL, sgASH2L Target 1, and sgASH2L Target 2 were all significantly different from the non-injected controls (p=0.02, Figure 3.3, Table 3.2). When sgNULL was compared with the sgASH2L Target 1 embryos no significant difference in blastocyst development was observed (p=0.12). A significant decrease in blastocyst rates was observed between sgNULL and sgASH2L Target 2 group (40.3 ± 3.0% vs 31.9 ± 2.1%, respectively, p=0.03). Morphology of blastocyst embryos in each treatment groups were of similar stage and quality on Day 8 (Figure 3.4).

Treatment	Number Cultured	Number Cleaved	Percent Cleaved	Number Blastocyst	Percent Blastocyst
Control	159	144	91.0 ± 1.5%[a]	79	49.1 ± 3.3%[a]
sgNULL	235	202	85.0 ± 3.0%[a]	94	40.3 ± 3.0%[b]
sgASH2L Target 1	185	159	85.0 ± 5.0%[a]	63	33.6 ± 5.0%[bc]
sgASH2L Target 2	191	170	87.0 ± 6.5%[a]	61	31.9 ± 2.1%[c]

Table 3.2 - Embryo development rates ± S.E.M for Control, sgNULL, sgASH2L Target 1 and sgASH2L Target 2 embryo groups. Values within a column with different superscripts are significantly different ($p < 0.05$)

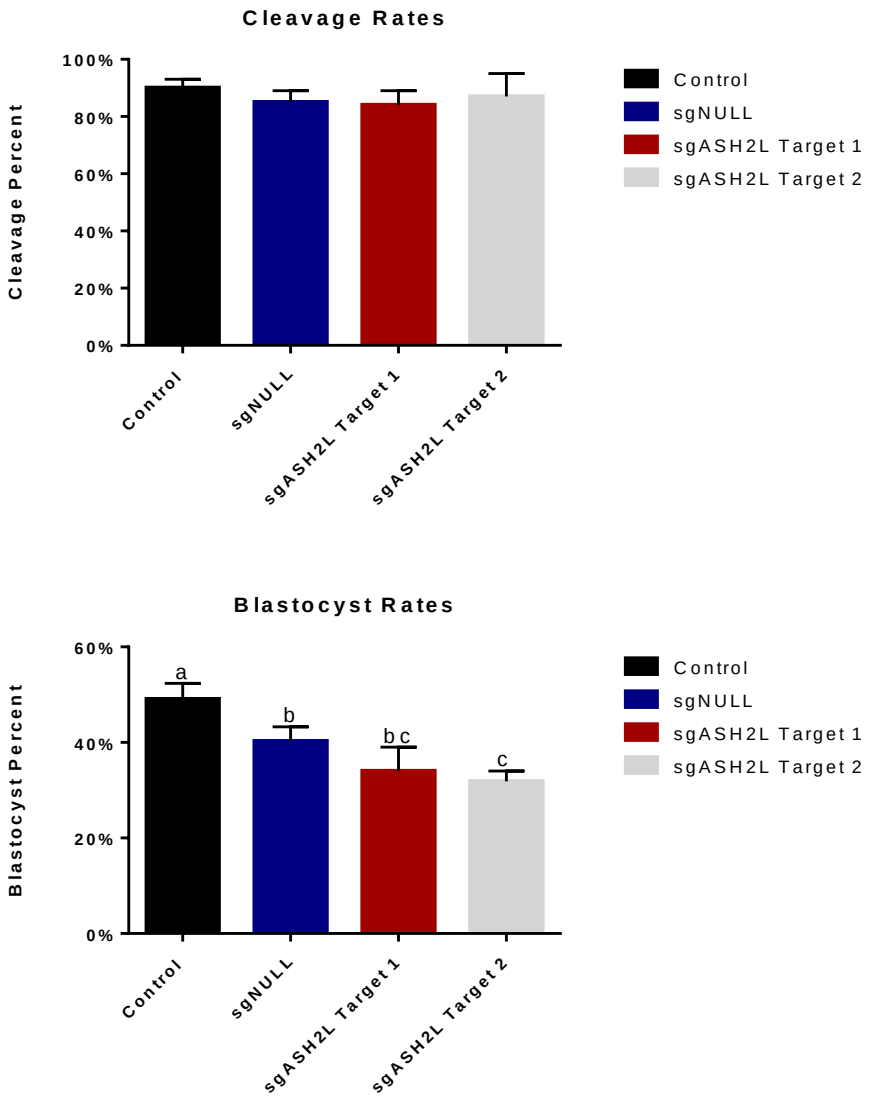

Figure 3.3 – Cleavage and blastocyst development rates for bovine embryos for the Control, siNULL, and sgASH2L embryo groups. Data was analyzed with a one-way ANOVA and Tukey HSD, alpha was set at 0.05. Significant difference between treatment groups is represented by a change in letter.

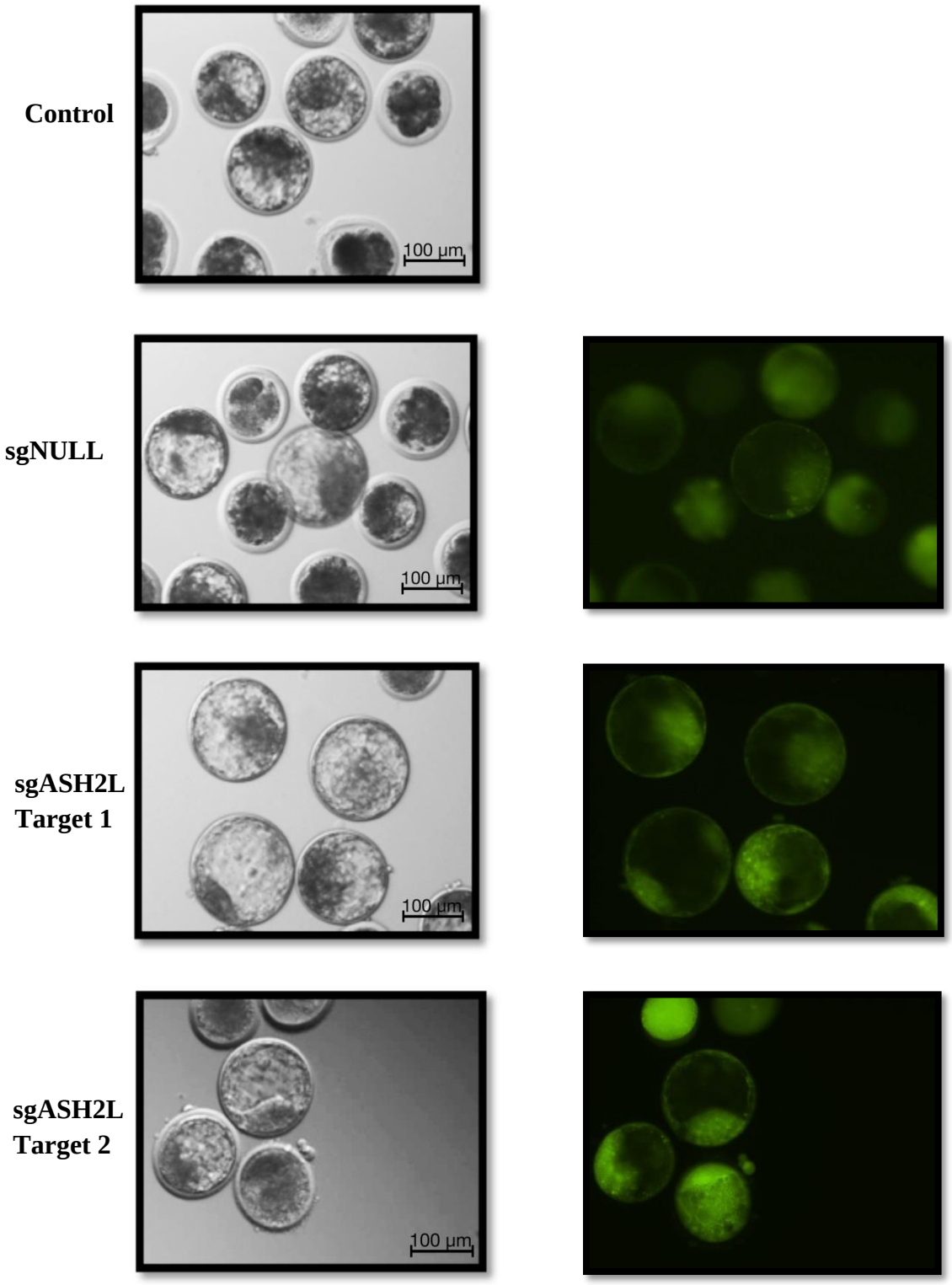

Figure 3.4 – Representative images for morphological analysis of blastocyst embryos on Day 8 of development. Bright field (20X) and flourescent photos (right) are shown in the sgNULL, sgASH2L Target 1 and sgASH2L Target 2 for confirmation of being microinjected.

ASH2L Expression Levels in Bovine Embryos

Embryos were examined at the 8-cell and blastocyst stage to see if the siRNAs were effective for suppressing ASH2L in the early embryo. Three biological replicates showed that the siRNAs targeting ASH2L reduced expression by 98% at the 8-cell stage and 82% at the blastocyst stage when compared to the sham-injected controls (P<0.0001, Figure 3.5).

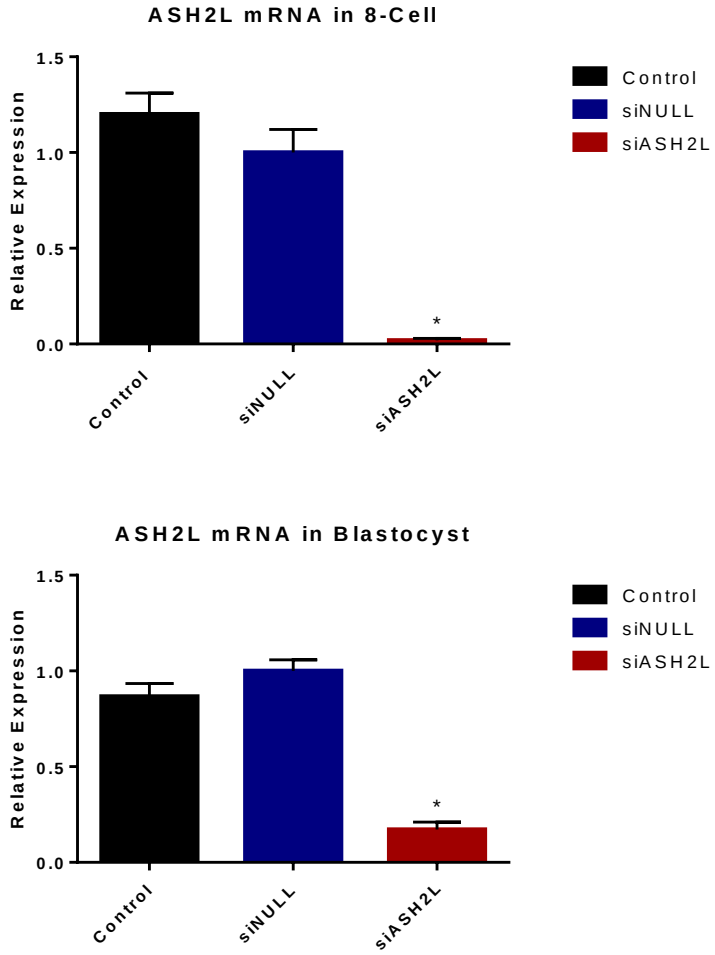

Figure 3.5 – ASH2L expression levels at the 8-cell and blastocyst stage in comparison to the Control and siNULL embryo groups. Data was analyzed with a one-way ANOVA and Tukey HSD, alpha was set at 0.05. Data observed to be significantly different from Control and siNULL groups is represented by *.

Immunocytochemistry

Analysis of 5mc and 5hmc

5mc and 5hmc levels were examined at the blastocyst stage to determine the effects of suppression of ASH2L in the early embryo. ICC analysis showed a significant increase in global cytosine methylation in the ASH2L suppressed embryo group when compared to the Control and siNULL embryos (0.35, 0.26, and 0.30, respectively, $P<0.01$, Figure 3.6). Hydroxymethlyation decreased in siASH2L embryos when matched with the non-injection and sham-injected controls (0.75, 0.93, and 0.87, respectively, $P<0.0001$,Table 3.3).

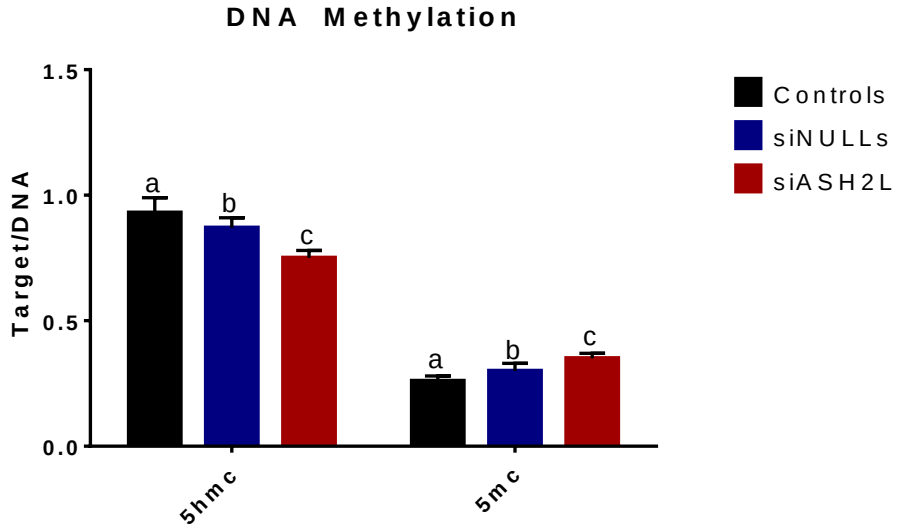

Figure 3.6 – ICC results of 5mc and 5hmc levels in blastocyst stage embryos for Control, siNULL, and siASH2L groups. Data was analyzed with a one-way ANOVA and Tukey HSD, alpha was set at 0.05. Significant difference between treatment groups is represented by a change in letter.

Primary Antibodies	Control	siNULL	siASH2L
5hmc	$0.93 \pm .02^{a}$	$0.87 \pm .02^{b}$	$0.75 \pm .01^{c}$
5mc	$0.26 \pm .01^{a}$	$0.30 \pm .02^{b}$	$0.35 \pm .01^{c}$
H3K4me2	$1.61 \pm .04^{a}$	$1.28 \pm .10^{b}$	$1.53 \pm .03^{c}$
H3K9me2-3	$0.71 \pm .01^{a}$	$0.69 \pm .01^{ab}$	$0.67 \pm .01^{b}$
H3K4me3	$0.57 \pm .02^{a}$	0.58 ± 02^{a}	$0.48 \pm .02^{b}$
H3K27me3	$0.53 \pm .01^{a}$	$0.54 \pm .02^{a}$	$0.62 \pm .02^{b}$

Table 3.3 **-** ICC results showing fluorescent intensity ratios with S.E.M. of DNA and histone methylation at the blastocyst stage of development. Different letters within a row indicate significant ($p<0.05$) difference between the groups.

Analysis of Posttranslational Histone Modifications

Blastocyst (N=425) from each treatment group were examined for posttranslational histone modifications by ICC. Depletion of ASH2L altered histone methylation levels with decreased levels of H3K4me3 (0.48, 0.57, and 0.58, $p<.0006$) and increased levels of H3K27me3 (0.62, 0.53, 0.54 $p<.001$) present in the siASH2L, Control and siNULL embryos, respectively (Figure 3.7, Table 3.3, and Figure 3.8). Depletion of ASH2L in the early embryo had no effect on H3K9me2-3 levels at the observed stage of development ($p=.16$). H3K4me2 levels were significantly altered due to injection of either the null siRNA or siASH2L, thus no meaningful interpretation of these data can be made. This may be due to increased non-specific fluorescence seen in the H3K4me2 embryos (Figure 3.9).

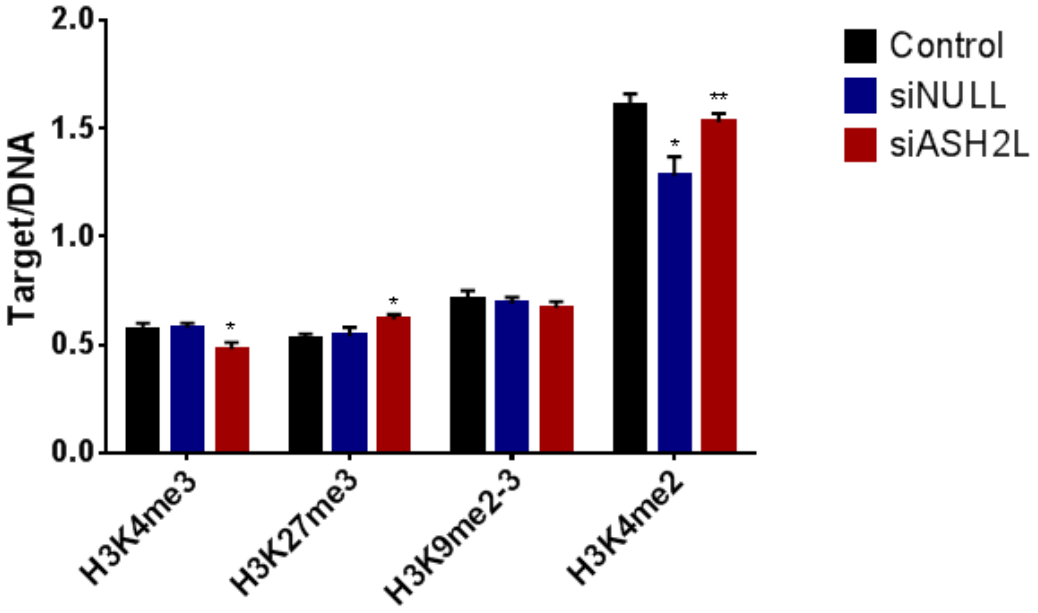

Figure 3.7 – ICC results analyzing histone methylation levels in blastocyst embryos in Control, siNULL, and siASH2L groups. Data was analyzed with a one-way ANOVA and Tukey HSD, alpha was set at 0.05. Significant difference from Control group is indicated by *. Significant difference from the Control and sgNULL group is represented by **.

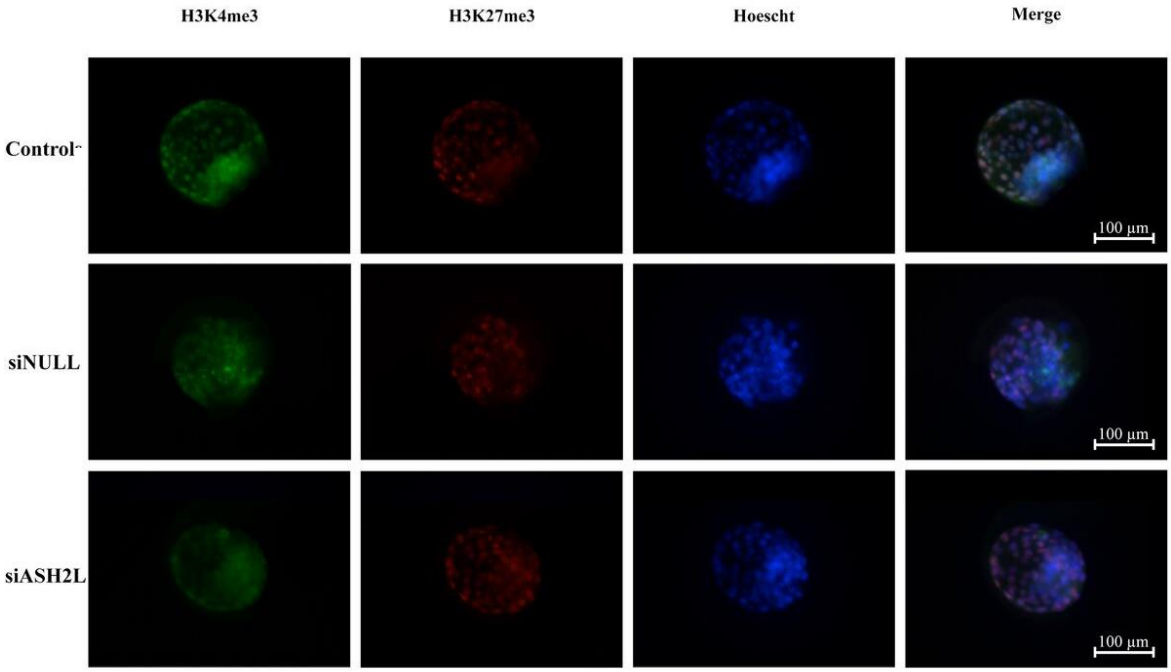

Figure 3.8 – ICC images of Day 7 blastocyst for the Control, siNULL, and siASH2L groups labeled for H3K4me3 and H3K27me3. Embryos stained and labeled images are for H3K4me3 (FITC), H3K27me3 (CY3), DNA (DAPI), and a merge of the three images.

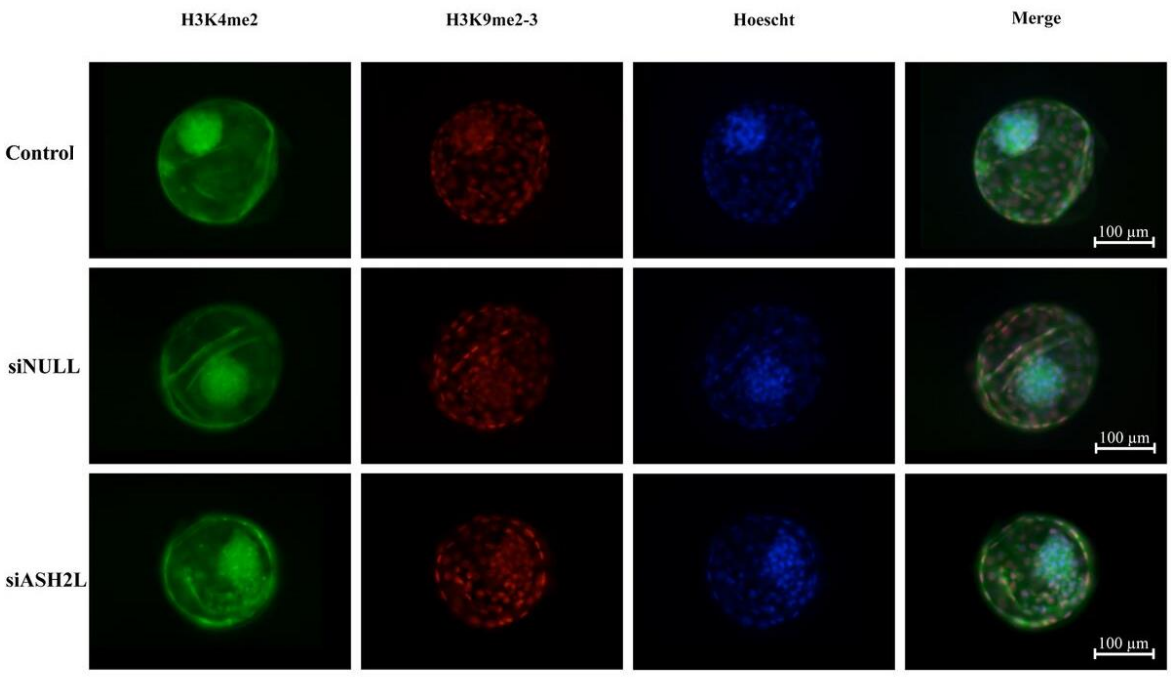

Figure 3.9 – ICC images of Day 7 blastocyst for the Control, siNULL, and siAHS2L groups labeled for H3K4me2 and H3K9me2-3. Embryos stained and labeled images are for H3K4me2 (FITC), H3K9me2-3 (CY3), DNA (DAPI), and a merge of the three images.

Preliminary Data of Targeted Mutations of ASH2L in Embryos

sgASH2L Target 1 Sequences

Individual sgASH2L Target 1 blastocysts were randomly selected from three different repilicates (N=20) and sequenced to observe if mutations were present in the ASH2L coding sequence. Observation of the targeted portion of the ASH2L gene sequenced showed the dual sgRNAs for the Target 1 site was 65% (13/20) effective for altering the ASH2L coding sequence (Figure 3.10). From the mutated embryos 69% (9/13) resulted in missense/silent mutation that caused no shift in the coding sequence. The remaining four mutated embryos resulted in either an in-frame or frameshift mutation. Two embryos were suggested to have a biallelic frameshift mutations that would suggest disruption to the ASH2L coding sequence for Exon 1. Further sequence analysis of reverse strand is needed to confirm this result.

```
WT Seq GGACCAGGCCCGGCAGCAGCTGCTAATGCAACACCGGCAGAAGAAGGGGAGACGAAGCAGGCAG
1AG1-2 GGACCAGGCCCGGCAGCtGCTGCTAATGCAACACCGGCAGAAGAAGGGGAGACGAAGCAGGCAG     Δ
1AG1-3 GGACCAGGCCCGGaAGCAGCTGCTAATGCAACACCGGCAGAAGAAGGGGAGACGAAGCAGGCAG     Δ
1AG1-4 GGACCAGGCCCGGCAGCAGCTGCTAATGCAACACCGGCAGAAGAAGGGGAGACGAAGCAGGCAG    WT
1AG1-5 GGACCATGCCCtGCAGCAGCTGCTAATGCAACACCGGCAGAAGAAGGGGAGACGAAGCAGGCAG     Δ
1AG1-6 GGACCAGGCCCGGCAGCAGCTGCTAATGCAACACCGGCAGAAGAAGGGGAGACGAAGCAGGCAACAG +3
1AG1-7 GGAACGGGCCCGGCAGCAGCTGCTAATGCAACACCGGCAGAAGAAGGGGAGACGAAGCAGGCAG     Δ
1AG1-8 GGACCAGGCCCGGCAGCAGCTGCTAATGCAACACCGGCAGAAGAAGGGGAGACGAAGCAGGCAG    WT
2AG1-1 GGAaC--GTGCCCGGCCTGC--CTGCTAATGAAACACCGGCAGAAGAAGGGGAaACtAAcCAGGCAG -1
2AG1-2 GGACCATGCCCtGCAGCAGCTGCTAATGCAACACCGGCAGAAGAAGGGGAGACGAAGCAGGCAG     Δ
2AG1-3 GGACCcGGCCCGGCAGCtGCTGCTAATGCAACACCGGCAGAAGAAGGGGAGACGAAGCAGGCAG     Δ
2AG1-4 GGACCAGGCCCGGCAGCAGCTGCTAATGCAACACCGGCAGAAGAAGGGGAGACtAAGCAGGCAG     Δ
2AG1-5 GGACCAGGCCCGGCAGCAGCTGCTAATGCAACACCGGCAGAAGAAGGGGAGACGAAGCAGGCAG    WT
2AG1-6 GGACCAGGCCCGGCAGCAGCTGCTAATGCAACACCGGCAGAAGAAGGGGAGACGAAGCAGGCAG    WT
2AG1-8 GGAaC--GtGCCCGGCCTCAGCTGCTAATGCAACACCGGCAGAAGAAGGGGAGACGAAGCAG---G  -3
3AG1-1 GGACCAGtCCCGGCAGCAGCTGCTAATGCAACACCGGCAGAAGAAGGGGAGACGAAGCAGGCAG     Δ
3AG1-2 GGACCAGGCCCGGCAGCAGCTGCTAATGCAACACCGGCAGAAGAAGGGGAGACGAAGCAGGCAG    WT
3AG1-4 GG-CC----------GCAGCTGCTAATGTC-ACACCGGCAGAAGAAGGGGAGACGAAGCAGGCAG  -11
3AG1-5 GGACCAGGCCCGGCAGCAGCTGCTAATGCAACACCGGCAGAAGAAGGGGAGACGAAGCAGGCAG    WT
3AG1-7 GGACCAGGCCCGGCCA-CAGCTGCTAATGCAACACCGGCAGAAGAAGGGGAGACGAAtCAGGCAG    Δ
3AG1-9 GGACCAGGCCCGGCAGCAGCTGCTAATGCAACACCGGCAGAAGAAGGGGAGACGAAGCAGGCAG    WT
```

Figure 3.10 – Sequence results from Day 8 embryos targeted with the first site of the CRISPR-Cas9 cascade. Green letters represent the PAM sequences for the target sites of the sgRNAs. Red letters indicate were the mutations are present with lower case letters representing a monoallelic mutation with capital letters representing a biallelic mutation. Right column shows change in coding sequence is present with Δ represents a mutation that did not result in change to the coding sequence. WT represents that the wild type sequence was present.

sgASH2L Target 2 Sequences

Individual blastocyst from the sgASH2L Target 2 group were randomly selected from three different repilicates (N=21) and the targeted portion of the ASH2L gene sequenced to examine if mutations were present (Figure 3.11). The overall targeting efficiency for the dual guides for the Target 2 site was 48% (10/21). From the ten mutations, seven resulted in what is a suggested biallelic frameshift mutations that would suggest by a chromatograph a disruption of the coding sequence in Exon 12. Further sequence analysis of the complementary strand is needed in order to confirm this preliminary result. The other three mutations caused a single nucleotide polymorphism (SNP) that would cause no shift in the coding sequence.

```
WT Seq ATTGGCAAACACTACTCTTCTGGCTACGGACAGGGAGACGTCCTGGGATTTTATATCAACC
1AG2-1 ATTGGCAAACACTACTaTTCTGGCTACGGACAGGGAGACGTCCTGGGATTTTATATCAACC        Δ
1AG2-2 ATTGGCAAACACTACTaTcCTGGCTACGGACAGGGAGACGTCCCTGGGATTTTATATCAACC      +1
1AG2-3 ATTGGCAAACACTACTCTTCTGGCTACGGACAGGGAGACGTCCTGGaAATTTTATATCAACC     +1
1AG2-4 ATTGGCAAACACTACTCTTCTGGCTACGGACAGGGAGACGTCCTGGGATTTTATATCAACC       WT
1AG2-6 ATTGGCAAACACTACTCTTCTGGCTACGGACAGGGAGACGTCCTGGGATTTTATATCAACC       WT
1AG2-8 ATTGGCAAACACTACTACTTACTGGCTACGGACAGGGAGACGTGGCCTGGGATTTTATATACAACC  +4
2AG2-2 ATTGGCAAACACTACTCTTACTGGCTACGGACAGGGAGGACGTgCGGTGGGATT--ATATATtAACC +1
2AG2-3 ATTGGCAAACACTACTCTTCTGGCTACGGACAGGGAGACGTCCTGGGATTTTATATCAACC       WT
2AG2-5 ATTGGCAAACACTACTCTTCTGGCTACGGACAGGGAGACGTCCTGGGATTTTATATCAACC       WT
2AG2-7 ATTGGCAAACgCTACTCTTCTGGCTACGGACAGGGAGACGTCCTGGGATTTTATATCAACC       Δ
2AG2-8 ATTGGCAAACACTACTCTTCTGGCTACGGACAGGGAGACGTCCTGGGATTTTATATCAACC       WT
2AG2-9 ATTGGCAAACACTACTCTTCTGGCTACGGACAGGGAGACGTCCTGGGATTTTATATCAACC       WT
3AG2-1 ATTGGCAAACACTACTCTTCTGGCTATGGACAGGGAGACGTCCTGGGATTTTATATCAACC       Δ
3AG2-2 ATTGGCAAACACTACTCTTCTGGCTACGGACAGGGAGACGTCCTGGGATTTTATATCAACC       WT
3AG2-3 ATTGGCAAACACTACTCTTCTGGCTACGGACAGGGAGACGTCCaGTGGGATTTTATATACAACC   +2
3AG2-4 ATTGGCAAACACTACTCTACTGGCTACGGACAGGGAGACGTCCTGGc-TTTTATATCAACC      -1
3AG2-5 ATTGGCAAACACTACTCTTCTGGCTACGGACAGGGAGACGTCCTGGGATTTTATATCAACC       WT
3AG2-6 ATTGGCAAACACTACTCTTCTGGCTAACGGACAGGGAGACGTCCTGGGATTTTATATCAACC     +1
3AG2-8 ATTGGCAAACACTACTCTTCTGGCTACGGACAGGGAGACGTCCTGGGATTTTATATCAACC       WT
3AG2-9 ATTGGCAAACACTACTCTTCTGGCTACGGACAGGGAGACGTCCTGGGATTTTATATCAACC       WT
```

Figure 3.11 – Sequence results from Day 8 embryos targeted with the second site of the CRISPR-Cas9 cascade. Green letters represent the PAM sequences for the target sites of the sgRNAs. Red letters indicate were the mutations that are present with lower case letters representing a monoallelic mutation with capital letters representing biallelic mutation. Right column show change in coding sequence is present with Δ representing a mutation that did not result in change to the coding sequence. WT represents that the wild type sequence was present.

Day 17 Conceptus Collection Morphology

On Day 17, conceptuses were collected from the siNULL and siASH2L transfers groups. The overall recovery rate from the siASH2L embryos transferred was 58.3% (7/12), while the siNULL recovery rate was 56.3% (9/16). Conceptuses collected from both treatment groups had an intact embryonic disc and also shown to be elongated at this point in developement (Figure 3.12 and 3.13). Variation in size of the filamentous conceptus was observed with both treatment groups.

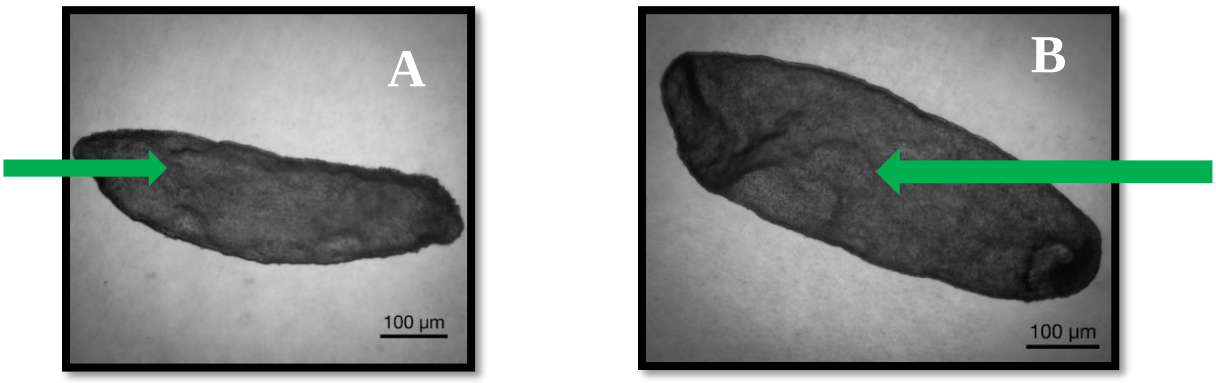

Figure 3.12 - Representative images of early elongation Day 17 conceptuses from the siNULL (A) and siASH2L (B) collected conceptuses. Green arrow points to embryonic disc that is intact in the preimplanted embryos.

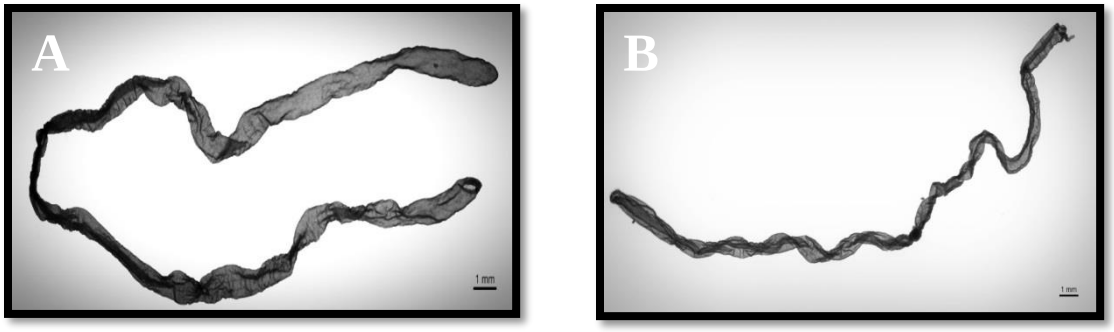

Figure 3.13 – Representative images of elongated Day 17 conceptus from the siNULL (A) and siASH2L (B) collected conceptuses.

RNA-Seq Data

RNA was collected from Day 17 conceptuses from the siNULL (N=3) and siASH2L (N=4) groups. These conceptuses were analyzed for global transcript profiles by RNA-Seq. Embryos of similar morphological appearance were compared with from the siNULL and siASH2L embryos during RNA-seq analysis. RNA-seq data showed the suppression of ASH2L by siRNA injection of zygotes resulted in altered gene expression profiles on Day 17 conceptuses (Table 3.4). Genes that were the most significantly altered were examined for common cell lineages in the Day 17 conceptus (Table 3.5). The BMP pathway was discovered to have significantly altered transcript levels present that originate from mesenchymal stem cells present in the Day 17 embryo.

Gene	Exp. Value Up Regulated	Gene	Exp. Value Down Regulated
SLC27A6	7.173	**CCL27**	-4.636
ZFP3	6.041	**AQP3**	-3.709
FAM213A	2.873	**CALB1**	-3.453
PAGE4	2.374	**PCK1**	-3.245
GAL3ST2	2.184	**GPX2**	-3.170
EEF1A1	1.999	**S100A1**	-2.893
ZNF521	1.983	**SLC38A5**	-2.846
PKD2L1	1.957	**LFITM7**	-2.807
SLC16A9	1.830	**VCAN**	-2.564
DLX5	1.784	**WNT11**	-2.563

Table 3.4 – Genes most significantly up and down regulated due to the suppression of ASH2L in the Day 17 conceptuses.

Transcriptional Changes in Day 17 Conceptuses (siNULL vs siASH2L)	Upregulated Genes	Down Regulated Genes
	109	**318**

Table 3.5- Number of genes altered in gene expression when compared to siNULL conceptuses ($p<0.05$).

RNA-Seq Validation

RNA-seq showed abnormal gene expression patterns present in mesynchymal stem cells. The mRNA expression levels of ZFP3, ZNF521, DLX5, CCL27, and WNT11 were examined via RT-qPCR in order to validate the RNA-seq expression results. Gene expression analysis showed that ZNF521 and DLX5 were significantly increased in siASH2L when compared to siNULL conceptuses (P=0.023 and P=0.033, respectively, Figure 3.14). No significant difference was observed with ZFP3 (P=0.303). Changes in CCL27 and WNT11 were not observed in mRNA expression analysis.

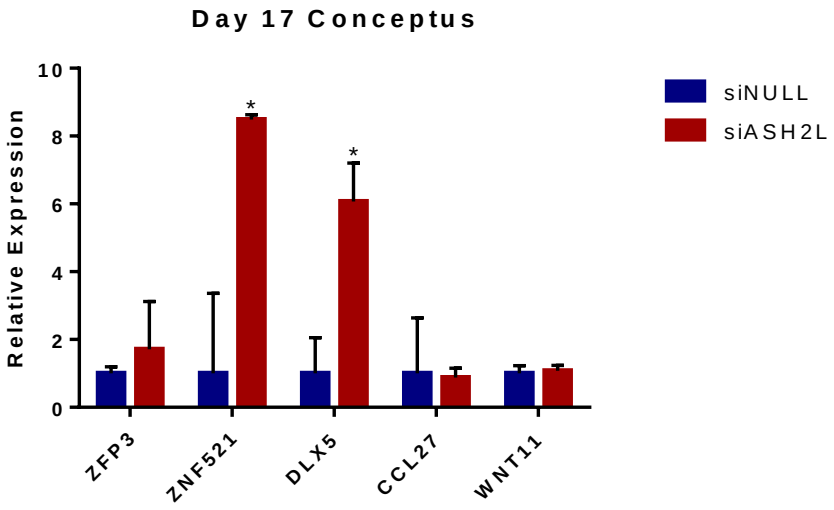

Figure 3.14 – Relative gene expression of genes associated with the BMP pathways in siNULL and siASH2L conceptuses. Data was analyzed with a one-way ANOVA and Tukey HSD, alpha was set at 0.05. Data that was observed to be significantly different from siNULL group is represented by *.

CHAPTER IV

CONCLUSIONS

Introduction

We hypothesized that depletion or deletion of ASH2L in bovine zygotes would alter preimplantation development, epigenetic reprogramming, gene expression, and result in morphological differences in the early bovine embryo. Results showed that reduction or removal of ASH2L did not inhibit blastocyst development. Further investigation found that suppression of ASH2L showed no morphological variation from sham-injected controls on Day 17. This result suggests that suppression of ASH2L in the early embryo does not have a detrimental effect on development during the preimplantation period.

We investigated epigenetic modifications in the ASH2L depleted embryos and found abnormal DNA and histone methylation patterns were present. Transcriptome analysis of the Day 17 conceptuses showed altered gene expression profiles that resulted from suppression of ASH2L in the early embryo. Even though these embryos appeared to be morphologically and developmentally competent, chromatin modifications and gene expression on Day 17 suggest otherwise. These findings propose that reduction of ASH2L during the reprogramming period of the embryo would have a detrimental effect later during post-implantation development.

Embryo Development for RNA Interference

Suppression of ASH2L did not alter cleavage and blastocyst development in the early embryo. When comparing these results with other HMTs and DNMTs, ASH2L was the only gene studied, when suppressed, did not alter development up to the blastocyst stage [107-111]. This result in the bovine is comparable to a study in mice that showed ASH2L-null embryos were viable at the blastocyst stage [125]. It also suggests that histone modifications associated with ASH2L may not play a necessary role during this developmental period.

With low expression levels of ASH2L present in bovine embryos, it is not an exact comparison to the mouse study. The low level of transcripts present suggest that some ASH2L protein is being produced in the early embryo. Analysis of ASH2L protein expression in the early bovine embryo would be ideal to further validate this assumption. However, this is not an option as there are no commercially produced antibodies that effectively target bovine ASH2L. To have a more comparable model to the ASH2L-null mouse, a knockout of ASH2L in the bovine embryo is needed to see if the technical limitations from RNA interference allowed for continuation of development [89].

CRISPR Embryo Development and Sequencing

To create a bovine model similar to what was previously used in mice, we utilized the CRISPR-Cas9 approach to target the bovine ASH2L coding sequence. The preliminary data from the sequence analysis comfirmed we were able to create mutations in the coding sequence as previously seen in other mammals using CRISPR-Cas9 [89, 129-131]. The suggested double strand break caused by Cas9 was repaired by the error prone repair mechanism of NHEJ that resulted with InDels being present [132, 133]. A portion of these

InDels caused a frameshift mutation thus disrupting the function of the ASH2L protein. Embryos with the suggested biallelic frameshift mutations still developed to the blastocyst stage, which is comparable to results reported with ASH2L-null mice [123]. Sequence analysis of the reverse stand would need to be performed in order to confirm that the double strand mutations are present.

With the sgASH2L Target 1 group, the majority of the sequences had missense or silent mutations present, which may not cause a change in protein function. Mutations from the sgASH2L Target 2 were advocated to have more biallelic frameshift mutations, but were less efficient at targeting the coding sequence. Selection of competent sgRNAs has become an increased area of research for increasing the efficiency of CRISPR-Cas9 and is similar to that previously seen with RNA interference [134-136]. Since the targeting efficiency for CRISPR-Cas9 was not 100% effective, we reverted back to the RNA interference approach for the rest of the studies analyzing the role of ASH2L during preimplantation development.

The sgRNAs used to target site 2 in the ASH2L gene resulted in a small but significant reduction in blastocyst development. The lower blastocyst rates from the sgASH2L Target 2 group can be explained by a couple of different possibilities. One could be off-target effects that are sometimes observed with CRISPR-Cas9 studies [137, 138]. It has been shown that off-targeting effects can happen with mismatches of up to 5 nucleotides upstream of the seed sequence for the sgRNA [139]. The other possibility could be from impurities present during preparation of the sgRNAsthat were used for microinjections. Any impurity or osmolarity change in the injection buffer could alter development of the early embryo.

Epigenetic Modifications

Similar to studies in mice, the suppression of ASH2L in the early embryo resulted in a global decrease of H3K4me3 levels in the blastocyst embryos [115]. This suggest that an altered gene transcription profile would be present in the ASH2L depleted blastocyst with numerous studies showing H3K4me3 having a role on facilitating a transcriptionally permissive chromatin status [100, 101]. Abnormal histone methylation patterns were also observed with the decease of H3K27me3 levels in the ASH2L suppressed embryo.

We observed H3K4me2 levels were significantly different from both the Control and siNULL embryos at the blastocyst stage. However, these altered levels of H3K4me2 are likely caused by problems with nonspecific binding of the primary antibody that leads to overstaining of secondary antibody, causing variation in fluorescent intensity levels. The reason for the nonspecific binding may have been due to the blocking buffer not being optimized for the primary polyclonal antibody produced in goat verses the other monoclonal antibodies utilized in these studies.

Even with the observed changes in histone methylation, the siASH2L embryos still developed comparably to the Control and siNULL embryos. The altered epigenetic status shows these changes did not result in embryonic lethality at this point in development. It also advocates that H3K4me3 may not play as critical role during the early developmental stages of the embryo. A previous study in Drosopila, has showed H3K4me3 levels are higher in stably expressed genes when compared to actively expressed genes [140]. This study suggests that ASH2L when regulating H3K4me3 levels may not facilitate active gene expression patterns as we had previously hypothesized during preimplantation development.

Altered DNA methylation patterns were present in ASH2L suppressed and NULL injected embryos at the blastocyst stage. This shows that even the micromanipulation methods that were utilized reformed the methylation status of the early embryo. With the ASH2L suppressed group, it was observed that these abnormal methylation patterns were more prevalent in the bovine blastocyst. It has been shown that an increase in DNMT3a was present when H3K4me3 was absent in mammalian cells [141]. Previous studies have also shown that the Polycomb group can mediate recruitment of DNA methyltransferases by regulation of H3K27me3 [142]. The altered histone methylation patterns are thus likely cause for the decrease in hydroxymethylation that is present in the ASH2L depleted blastocysts.

Day 17 Embryo Collections

Since it was previously observed that suppression of ASH2L did not alter development to the blastocysts stage, it would be advantageous to examine siASH2L embryos later in development. Previous studies in mice suggest ASH2L suppressed embryos would not be viable after the blastocyst stage since ASH2L-null embryos were nonviable between the blastocyst stage and mid gestation [123]. Collection of the Day 17 conceptuses showed suppression of ASH2L did not inhibit development of the embryonic disc and elongation of the conceptus. The ASH2L embryos did have various lengths of filamentous conceptuses at this point in development. The altered elongation patterns were present in both siNULL and siASH2L conceptus groups thus suggesting it is caused by the maternal environment. It has been shown when high levels of progesterone are present in the maternal uterine environment, elongation of conceptus occurs more rapidly when compared to lower

levels [143, 144]. These findings show that the suppression of ASH2L did not alter morphological development of the conceptus before binding to the uterine epithelium.

RNA-Seq and Validation

As we hypothesized, abnormal gene expression profiles were present in the Day 17 conceptus due to the suppression of ASH2L in the early embryo. The most significantly up and down regulated RNA-seq data showed abnormal transcripts were present in the BMP and TGF-beta pathways that arise from mesenchymal stem cells present in the Day 17 conceptus [145]. This was validated by RT-qPCR, that showed abnormal gene expression patterns were higher, when compared to control group, for ZNF521 and DLX5. The altered mRNA expression levels for these genes were consistent with the RNA-seq data. When these messenchymal stem cells begin to differention they form osteocytes, chondrocyts, that are responsible for making cartilage and bone [146, 147]. To see if this would has an effect on pregnancy, embryos depleted of ASH2L in the early embryo would need to develop past Day 17 conceptus. ZNF521 and DLX5 have also been shown to be expressed in trophoblastic cells that form into the placenta [148]. DLX5 is also a maternally expressed gene that has been shown to be abnormally methylated and mRNA expression upregulated in preclamptic placentas of humans [149, 150]. The effect of overexpression of DLX5 in the bovine placenta has yet to be studied. No effect was observed with other imprinting genes due to the suppression of ASH2L in the Day 17 conceptus.

No change in gene expression was observed in RNA-seq validation of ZFP3, CCL27, and WNT11. In control embryos, expression levels were examined in comparison to reference genes (Figure A9). This showed lower expression levels were present in the genes

than those that were validated by RT-qPCR. It has been shown that RNA-seq is more sensitive and can detect low level transcripts [151]. This shows that the altered transcriptome profile that was observed with RNA-seq not have as wide spread outcome as previously thought.

It was previously shown that ASH2L played a role in HOX gene expression by increasing the trimethylation of H3K4me3 [118, 119]. Altered histone methylation patterns of H3K27me3 and H3K4me3 were present in blastocysts suppressed for ASH2L and was suggested to have an inhibitory effect on HOX gene expression during embryonic development. Studies have shown H3K27me3, via the PcG, and H3K4me3, by way of TrxG, are associated with HOX gene expression of the early embryo [152, 153]. This change in HOX gene expression suggests that phenotypic abnormalities would be present later in development [154]. However, we did not observe drastic alterations in HOX gene expression patterns were present in the Day 17 conceptus. Studies in mice have showed that HOX gene expression was higher in mid gestation (Day 10.5-16.5) [155]. These findings in mice would suggest that HOX gene expression would be more prevalent later in development.

Summary

To characterize the role of ASH2L, we examined whether depletion or deletion of ASH2L would alter preimplantation development, embryo morphology, epigenetic reprogramming, and gene expression. Developmental data showed the suppression or deletion of ASH2L in the early embryo did not affect the developmental potential to the blastocyst stage during *in vitro* development. Embryos from both studies had morphology that suggested good quality blastocysts in accordance to IETS guidelines. Furthermore, the

ASH2L suppressed embryos continued development throughout preimplantation and on Day 17 no morphological variances were observed when compared to respective controls.

More in depth analysis of ASH2L depleted embryos showed abnormal distribution of cytosine and histone methylation patterns at the blastocyst stage. This altered epigenetic state suggested a chromatin status that does not facilitate transcription and would alter gene expression later in development. It also questions the role of H3K4me3 in the early embryo due to the decrease levels present in the ASH2L suppressed embryos. Transcriptome analysis of ASH2L suppressed conceptuses showed altered gene transcriptome profiles were present that are associated with mesenchymal stem cells on Day 17. These findings suggest that the suppression of ASH2L in the early embryo altered gene expression associated with stem cells and this could have an effect later during post-implantation development. These findings show alteration to normal ASH2L levels in the early embryo could be a link to inferior embryos that arise from IVP.

REFERENCES

1. Brackett, B.G., et al., *Normal development following in vitro fertilization in the cow*. Biol Reprod, 1982. **27**(1): p. 147-158.

2. Hasler, J.F., *In-vitro production of cattle embryos: Problems with pregnancies and parturition.* Hum Reprod, 2000. **15 Suppl 5**: p. 47-58.

3. Hasler, J.F., *Forty years of embryo transfer in cattle: A review focusing on the journal Theriogenology, the growth of the industry in North America, and personal reminisces.* Theriogenology, 2014. **81**(1): p. 152-169.

4. Pontes, J.H.F., et al., *Comparison of embryo yield and pregnancy rate between in vivo and in vitro methods in the same Nelore (Bos indicus) donor cows.* Theriogenology, 2009. **71**(4): p. 690-697.

5. Enright, B.P., et al., *Culture of in vitro produced bovine zygotes in vitro vs in vivo: Implications for early embryo development and quality.* Theriogenology, 2000. **54**(5): p. 659-673.

6. Wells, D.N., P.M. Misica, and H.R. Tervit, *Production of cloned calves following nuclear transfer with cultured adult mural granulosa cells.* Biol Reprod, 1999. **60**(4): p. 996-1005.

7. Hill, J.R., et al., *Evidence for placental abnormality as the major cause of mortality in first-trimester somatic cell cloned bovine fetuses.* Biol Reprod, 2000. **63**(6): p. 1787-1794.

8. Wilson, J.M., et al., *Comparison of birth weight and growth characteristics of bovine calves produced by nuclear transfer (cloning), embryo transfer and natural mating.* Animal Reproduction Science, 1995. **38**(1–2): p. 73-83.

9. Young, L.E., K.D. Sinclair, and I. Wilmut, *Large offspring syndrome in cattle and sheep.* Rev Reprod, 1998. **3**(3): p. 155-163.

10. Farin, P.W., J.A. Piedrahita, and C.E. Farin, *Errors in development of fetuses and placentas from in vitro-produced bovine embryos.* Theriogenology, 2006. **65**(1): p. 178-191.

11. Farin, C.E., P.W. Farin, and J.A. Piedrahita, *Development of fetuses from in vitro–produced and cloned bovine embryos.* Journal of Animal Science, 2004. **82**(13_suppl): p. E53-62.

12. Leridon, H., *Can assisted reproduction technology compensate for the natural decline in fertility with age? A model assessment.* Hum Reprod, 2004. **19**(7): p. 1548-1553.

13. Soejima, H. and K. Higashimoto, *Epigenetic and genetic alterations of the imprinting disorder Beckwith-Wiedemann syndrome and related disorders.* J Hum Genet, 2013. **58**(7): p. 402-409.

14. Wang, J. and M.V. Sauer, *In vitro fertilization (IVF): A review of 3 decades of clinical innovation and technological advancement.* Ther Clin Risk Manag, 2006. **2**(4): p. 355-364.

15. Gicquel, C., et al., *In vitro fertilization may increase the risk of Beckwith-Wiedemann syndrome related to the abnormal imprinting of the KCN1OT gene.* Am J Hum Genet, 2003. **72**(5): p. 1338-1341.

16. Ludwig, M., et al., *Increased prevalence of imprinting defects in patients with Angelman syndrome born to subfertile couples.* J Med Genet, 2005. **42**(4): p. 289-91.

17. Weksberg, R., C. Shuman, and J.B. Beckwith, *Beckwith-Wiedemann syndrome.* Eur J Hum Genet, 2010. **18**(1): p. 8-14.

18. Gicquel, C., A. El-Osta, and Y. Le Bouc, *Epigenetic regulation and fetal programming.* Best Pract Res Clin Endocrinol Metab, 2008. **22**(1): p. 1-16.

19. Driver, A.M., et al., *RNA-Seq analysis uncovers transcriptomic variations between morphologically similar in vivo- and in vitro-derived bovine blastocysts.* BMC Genomics, 2012. **13**(1): p. 1-9.

20. Mann, M.R., et al., *Selective loss of imprinting in the placenta following preimplantation development in culture.* Development, 2004. **131**(15): p. 3727-3735.

21. Giraldo, A.M., et al., *Effect of epigenetic modifications of donor somatic cells on the subsequent chromatin remodeling of cloned bovine embryos.* Biol Reprod, 2008. **78**(5): p. 832-840.

22. Barros, S.P. and S. Offenbacher, *Epigenetics: Connecting environment and genotype to phenotype and disease.* J Dent Res, 2009. **88**(5): p. 400-408.

23. Holliday, R., *Epigenetics: A historical overview.* Epigenetics, 2006. **1**(2): p. 76-80.

24. Morange, M., *The relations between genetics and epigenetics: A historical point of view.* Ann N Y Acad Sci, 2002. **981**: p. 50-60.

25. Surani, M.A., *Reprogramming of genome function through epigenetic inheritance.* Nature, 2001. **414**(6859): p. 122-128.

26. Feil, R. and M.F. Fraga, *Epigenetics and the environment: Emerging patterns and implications.* Nat Rev Genet, 2011. **13**(2): p. 97-109.

27. Bird, A., *DNA methylation patterns and epigenetic memory.* Genes Dev, 2002. **16**(1): p. 6-21.

28. Jin, B., Y. Li, and K.D. Robertson, *DNA methylation: Superior or subordinate in the epigenetic hierarchy?* Genes Cancer, 2011. **2**(6): p. 607-617.

29. Li, E., C. Beard, and R. Jaenisch, *Role for DNA methylation in genomic imprinting.* Nature, 1993. **366**(6453): p. 362-365.

30. Monk, M., M. Boubelik, and S. Lehnert, *Temporal and regional changes in DNA methylation in the embryonic, extraembryonic and germ cell lineages during mouse embryo development.* Development, 1987. **99**(3): p. 371-382.

31. Jones, P.A. and D. Takai, *The role of DNA methylation in mammalian epigenetics.* Science, 2001. **293**(5532): p. 1068-1070.

32. Miller, O.J., et al., *5-Methylcytosine localised in mammalian constitutive heterochromatin.* Nature, 1974. **251**(5476): p. 636-637.

33. Jones, P.A., *Functions of DNA methylation: Islands, start sites, gene bodies and beyond.* Nat Rev Genet, 2012. **13**(7): p. 484-492.

34. Medvedeva, Y.A., et al., *Effects of cytosine methylation on transcription factor binding sites.* BMC Genomics, 2014. **15**(1): p. 1-12.

35. Lander, E.S., et al., *Initial sequencing and analysis of the human genome.* Nature, 2001. **409**(6822): p. 860-921.

36. Farthing, C.R., et al., *Global mapping of DNA methylation in mouse promoters reveals epigenetic reprogramming of pluripotency genes.* PLoS Genet, 2008. **4**(6): p. 1-17.

37. Wan, J., et al., *Characterization of tissue-specific differential DNA methylation suggests distinct modes of positive and negative gene expression regulation.* BMC Genomics, 2015. **16**(1): p. 1-11.

38. Jin, B. and K.D. Robertson, *DNA methyltransferases, DNA damage repair, and cancer.* Adv Exp Med Biol, 2013. **754**: p. 3-29.

39. Okano, M., S. Xie, and E. Li, *Cloning and characterization of a family of novel mammalian DNA (cytosine-5) methyltransferases.* Nat Genet, 1998. **19**(3): p. 219-220.

40. Okano, M., et al., *DNA methyltransferases Dnmt3a and Dnmt3b are essential for de novo methylation and mammalian development.* Cell, 1999. **99**(3): p. 247-257.

41. Smallwood, S.A. and G. Kelsey, *De novo DNA methylation: A germ cell perspective.* Trends in Genetics. **28**(1): p. 33-42.

42. Young, L.E. and N. Beaujean, *DNA methylation in the preimplantation embryo: The differing stories of the mouse and sheep.* Animal Reproduction Science, 2004. **82–83**: p. 61-78.

43. Reik, W. and W. Dean, *DNA methylation and mammalian epigenetics.* Electrophoresis, 2001. **22**(14): p. 2838-2843.

44. Reik, W., *Stability and flexibility of epigenetic gene regulation in mammalian development.* Nature, 2007. **447**(7143): p. 425-432.

45. Latham, K.E., *Epigenetic modification and imprinting of the mammalian genome during development.* Curr Top Dev Biol, 1999. **43**: p. 1-49.

46. Mann, M.R. and M.S. Bartolomei, *Epigenetic reprogramming in the mammalian embryo: Struggle of the clones.* Genome Biol, 2002. **3**(2): p. 1003.

47. Wu, H. and Y. Zhang, *Mechanisms and functions of Tet protein-mediated 5-methylcytosine oxidation.* Genes Dev, 2011. **25**(23): p. 2436-2452.

48. Ito, S., et al., *Tet proteins can convert 5-methylcytosine to 5-formylcytosine and 5-carboxylcytosine.* Science, 2011. **333**(6047): p. 1300-1303.

49. Ito, S., et al., *Role of Tet proteins in 5mC to 5hmC conversion, ES-cell self-renewal and inner cell mass specification.* Nature, 2010. **466**(7310): p. 1129-1133.

50. Bourc'his, D., et al., *Delayed and incomplete reprogramming of chromosome methylation patterns in bovine cloned embryos.* Current Biology, 2001. **11**(19): p. 1542-1546.

51. Chen, T., et al., *The DNA methylation events in normal and cloned rabbit embryos.* FEBS Letters, 2004. **578**(1–2): p. 69-72.

52. Messerschmidt, D.M., B.B. Knowles, and D. Solter, *DNA methylation dynamics during epigenetic reprogramming in the germline and preimplantation embryos.* Genes Dev, 2014. **28**(8): p. 812-828.

53. Latham, K.E. and R.M. Schultz, *Embryonic genome activation.* Front Biosci, 2001. **6**: p. D748-759.

54. Reik, W. and J. Walter, *Genomic imprinting: Parental influence on the genome.* Nat Rev Genet, 2001. **2**(1): p. 21-32.

55. McGrath, J. and D. Solter, *Completion of mouse embryogenesis requires both the maternal and paternal genomes.* Cell, 1984. **37**(1): p. 179-183.

56. Bartolomei, M.S. and S.M. Tilghman, *Genomic imprinting in mammals.* Annu Rev Genet, 1997. **31**: p. 493-525.

57. Li, E., et al., *DNA methylation, genomic imprinting, and mammalian development.* Cold Spring Harb Symp Quant Biol, 1993. **58**: p. 297-305.

58. Guillomot, M., et al., *Abnormal Expression of the imprinted gene Phlda2 in cloned bovine placenta.* Placenta, 2010. **31**(6): p. 482-490.

59. Chen, Z., et al., *Large offspring syndrome: A bovine model for the human loss-of-imprinting overgrowth syndrome Beckwith-Wiedemann.* Epigenetics, 2013. **8**(6): p. 591-601.

60. Allfrey, V.G., R. Faulkner, and A.E. Mirsky, *Acetylation and methylation of histones and their possible role in the regulation of RNA synthesis.* Proc Natl Acad Sci U S A, 1964. **51**: p. 786-794.

61. Luger, K., et al., *Crystal structure of the nucleosome core particle at 2.8: A resolution.* Nature, 1997. **389**(6648): p. 251-260.

62. Richmond, T.J. and C.A. Davey, *The structure of DNA in the nucleosome core.* Nature, 2003. **423**(6936): p. 145-150.

63. Bannister, A.J. and T. Kouzarides, *Regulation of chromatin by histone modifications.* Cell Res, 2011. **21**(3): p. 381-395.

64. Luger, K. and T.J. Richmond, *The histone tails of the nucleosome.* Curr Opin Genet Dev, 1998. **8**(2): p. 140-146.

65. Strahl, B.D. and C.D. Allis, *The language of covalent histone modifications.* Nature, 2000. **403**(6765): p. 41-45.

66. Morgan, H.D., et al., *Epigenetic reprogramming in mammals.* Hum Mol Genet, 2005. **14 Spec No 1**: p. R47-58.

67. Feng, S., S.E. Jacobsen, and W. Reik, *Epigenetic reprogramming in plant and animal development.* Science, 2010. **330**(6004): p. 622-627.

68. Karimi, M.M., et al., *DNA methylation and SETDB1/H3K9me3 regulate predominantly distinct sets of genes, retroelements, and chimeric transcripts in mESCs.* Cell Stem Cell, 2011. **8**(6): p. 676-687.

69. Zhang, X., et al., *Genome-wide analysis of mono-, di- and trimethylation of histone H3 lysine 4 in Arabidopsis thaliana.* Genome Biol, 2009. **10**(6): p. R62.

70. Schuettengruber, B., et al., *Trithorax group proteins: Switching genes on and keeping them active.* Nat Rev Mol Cell Biol, 2011. **12**(12): p. 799-814.

71. Deal, R.B., J.G. Henikoff, and S. Henikoff, *Genome-wide kinetics of nucleosome turnover determined by metabolic labeling of histones.* Science, 2010. **328**(5982): p. 1161-1164.

72. Gellon, G. and W. McGinnis, *Shaping animal body plans in development and evolution by modulation of Hox expression patterns.* Bioessays, 1998. **20**(2): p. 116-125.

73. Block, K., et al., *In utero diethylstilbestrol (DES) exposure alters Hox gene expression in the developing mullerian system.* FASEB J, 2000. **14**(9): p. 1101-1108.

74. Seifert, A., et al., *Role of Hox genes in stem cell differentiation.* World J Stem Cells, 2015. **7**(3): p. 583-595.

75. Mallo, M. and C.R. Alonso, *The regulation of Hox gene expression during animal development.* Development, 2013. **140**(19): p. 3951-3963.

76. Golding, M.C. and M.E. Westhusin, *Analysis of DNA (cytosine 5) methyltransferase mRNA sequence and expression in bovine preimplantation embryos, fetal and adult tissues.* Gene Expr Patterns, 2003. **3**(5): p. 551-558.

77. Menezo, Y.J. and F. Herubel, *Mouse and bovine models for human IVF.* Reprod Biomed Online, 2002. **4**(2): p. 170-175.

78. Livesay, E.A. and U.G. Bee, *A study of the gestation periods of five breeds of cattle.* Journal of Animal Science, 1945. **4**(1) : p. 13-14.

79. Hardy, K., A.H. Handyside, and R.M. Winston, *The human blastocyst: Cell number, death and allocation during late preimplantation development in vitro.* Development, 1989. **107**(3): p. 597-604.

80. Latham, K.E., *Mechanisms and control of embryonic genome activation in mammalian embryos.* Int Rev Cytol, 1999. **193**: p. 71-124.

81. Mouse Genome Sequencing, C., et al., *Initial sequencing and comparative analysis of the mouse genome.* Nature, 2002. **420**(6915): p. 520-562.

82. Mazza, R., et al., *The other side of comparative genomics: Genes with no orthologs between the cow and other mammalian species.* BMC Genomics, 2009. **10**(1): p. 1-15.

83. Horrobin, D.F., *Modern biomedical research: An internally self-consistent universe with little contact with medical reality?* Nat Rev Drug Discov, 2003. **2**(2): p. 151-154.

84. Blokland, R.v., et al., *Transgene-mediated suppression of chalcone synthase expression in Petunia hybrida results from an increase in RNA turnover.* The Plant Journal, 1994. **6**(6): p. 861-877.

85. Fire, A., et al., *Potent and specific genetic interference by double-stranded RNA in Caenorhabditis elegans.* Nature, 1998. **391**(6669): p. 806-811.

86. Bernstein, E., et al., *Role for a bidentate ribonuclease in the initiation step of RNA interference.* Nature, 2001. **409**(6818): p. 363-366.

87. Sioud, M., *Engineering better immunotherapies via RNA interference.* Hum Vaccin Immunother, 2014. **10**(11): p. 3165-3174.

88. Shabalina, S.A. and E.V. Koonin, *Origins and evolution of eukaryotic RNA interference.* Trends Ecol Evol, 2008. **23**(10): p. 578-587.

89. Cong, L., et al., *Multiplex genome engineering using CRISPR/Cas systems.* Science, 2013. **339**(6121): p. 819-823.

90. Cong, L. and F. Zhang, *Genome engineering using CRISPR-Cas9 system.* Methods Mol Biol, 2015. **1239**: p. 197-217.

91. Hsu, P.D., E.S. Lander, and F. Zhang, *Development and applications of CRISPR-Cas9 for genome engineering.* Cell, 2014. **157**(6): p. 1262-1278.

92. Sander, J.D. and J.K. Joung, *CRISPR-Cas systems for editing, regulating and targeting genomes.* Nat Biotechnol, 2014. **32**(4): p. 347-355.

93. Wang, H., et al., *One-step generation of mice carrying mutations in multiple genes by CRISPR/Cas-mediated genome engineering.* Cell, 2013. **153**(4): p. 910-918.

94. Heyman, Y., et al., *Maintenance of the corpus luteum after uterine transfer of trophoblastic vesicles to cyclic cows and ewes.* J Reprod Fertil, 1984. **70**(2): p. 533-540.

95. Garrett, J.E., et al., *Evidence for maternal regulation of early conceptus growth and development in beef cattle.* Journal of Reproduction and Fertility, 1988. **84**(2): p. 437-446.

96. Maddox-Hyttell, P., et al., *Morphological assessment of preimplantation embryo quality in cattle.* Reprod Suppl, 2003. **61**: p. 103-116.

97. Satterfield, M.C., F.W. Bazer, and T.E. Spencer, *Progesterone regulation of preimplantation conceptus growth and galectin 15 (LGALS15) in the ovine uterus.* Biol Reprod, 2006. **75**(2): p. 289-296.

98. Mann, G.E., et al., *The regulation of interferon-tau production and uterine hormone receptors during early pregnancy.* J Reprod Fertil Suppl, 1999. **54**: p. 317-328.

99. Donaldson, L.E., *Matching of embryo stages and grades with recipient oestrous synchrony in bovine embryo transfer.* Vet Rec, 1985. **117**(19): p. 489-491.

100. Nash, J.M., et al., *Comparison of long- versus short-term CIDR-based protocols to synchronize estrus prior to fixed-time AI in postpartum beef cows.* Anim Reprod Sci, 2012. **132**(1-2): p. 11-16.

101. Lucifero, D., et al., *Bovine SNRPN methylation imprint in oocytes and day 17 in vitro-produced and somatic cell nuclear transfer embryos.* Biol Reprod, 2006. **75**(4): p. 531-538.

102. Rodriguez-Alvarez, L., et al., *Elongation and gene expression in bovine cloned embryos transferred to temporary recipients.* Zygote, 2009. **17**(4): p. 353-365.

103. Mamo, S., et al., *Conceptus-endometrium crosstalk during maternal recognition of pregnancy in cattle.* Biol Reprod, 2012. **87**(1): p. 6, 1-9.

104. Fischer-Brown, A.E., et al., *Embryonic disc development and subsequent viability of cattle embryos following culture in two media under two oxygen concentrations.* Reprod Fertil Dev, 2004. **16**(8): p. 787-93.

105. Golding, M.C., et al., *Histone-lysine N-methyltransferase SETDB1 is required for development of the bovine blastocyst.* Theriogenology, 2015. **84**(8): p. 1411-1422.

106. Snyder, M.D., et al., *122 Suppression of epigenetic modifiers alters the bovine embryonic developmental program during in vitro culture.* Reproduction, Fertility and Development, 2013. **26**(1): p. 175-175.

107. Golding, M.C., et al., *Examination of DNA methyltransferase expression in cloned embryos reveals an essential role for Dnmt1 in bovine development.* Mol Reprod Dev, 2011. **78**(5): p. 306-317.

108. Williamson, G.L., et al., *201 Suppression of Suz12 in bovine preimplantation embryos via cytoplasmic small interfering RNA injections.* Reproduction, Fertility and Development, 2010. **23**(1): p. 200-200.

109. Linger, G.D., et al., *189 Transcriptional profiling of histone-modifying genes during bovine pre-implantation embryo development in vitro.* Reproduction, Fertility and Development, 2008. **21**(1): p. 193-193.

110. Wu, L., et al., *ASH2L regulates ubiquitylation signaling to MLL: Trans-regulation of H3 K4 methylation in higher eukaryotes.* Mol Cell, 2013. **49**(6): p. 1108-1120.

111. Yokoyama, A., et al., *Leukemia proto-oncoprotein MLL forms a SET1-like histone methyltransferase complex with menin to regulate Hox gene expression.* Mol Cell Biol, 2004. **24**(13): p. 5639-5649.

112. Cao, F., et al., *An Ash2L/RbBP5 heterodimer stimulates the MLL1 methyltransferase activity through coordinated substrate interactions with the MLL1 SET domain.* PLoS One, 2010. **5**(11): p. 1-11.

113. Dou, Y., et al., *Regulation of MLL1 H3K4 methyltransferase activity by its core components.* Nat Struct Mol Biol, 2006. **13**(8): p. 713-719.

114. Patel, A., et al., *A novel non-SET domain multi-subunit methyltransferase required for sequential nucleosomal histone H3 methylation by the mixed lineage leukemia protein-1 (MLL1) core complex.* J Biol Chem, 2011. **286**(5): p. 3359-3369.

115. Steward, M.M., et al., *Molecular regulation of H3K4 trimethylation by ASH2L, a shared subunit of MLL complexes.* Nat Struct Mol Biol, 2006. **13**(9): p. 852-854.

116. Lee, J.E., et al., *H3K4 mono- and di-methyltransferase MLL4 is required for enhancer activation during cell differentiation.* Elife, 2013. **2**: p. 1-25.

117. Shilatifard, A., *The COMPASS family of histone H3K4 methylases: Mechanisms of regulation in development and disease pathogenesis.* Annu Rev Biochem, 2012. **81**: p. 65-95.

118. Tan, C.C., et al., *Transcription factor Ap2delta associates with Ash2l and ALR, a trithorax family histone methyltransferase, to activate Hoxc8 transcription.* Proc Natl Acad Sci U S A, 2008. **105**(21): p. 7472-7477.

119. Rampalli, S., et al., *p38 MAPK signaling regulates recruitment of Ash2L-containing methyltransferase complexes to specific genes during differentiation.* Nat Struct Mol Biol, 2007. **14**(12): p. 1150-1156.

120. Chen, Y., et al., *Crystal structure of the N-terminal region of human Ash2L shows a winged-helix motif involved in DNA binding.* EMBO Rep, 2011. **12**(8): p. 797-803.

121. South, P.F., et al., *A conserved interaction between the SDI domain of Bre2 and the Dpy-30 domain of Sdc1 is required for histone methylation and gene expression.* J Biol Chem, 2010. **285**(1): p. 595-607.

122. Chen, Y., et al., *Structure of the SPRY domain of human Ash2L and its interactions with RbBP5 and DPY30.* Cell Res, 2012. **22**(3): p. 598-602.

123. Stoller, J.Z., et al., *Ash2l interacts with Tbx1 and is required during early embryogenesis.* Exp Biol Med (Maywood), 2010. **235**(5): p. 569-576.

124. Barnard, R.J., et al., *Emergence of resistance-associated variants after failed triple therapy with vaniprevir in treatment-experienced non-cirrhotic patients with hepatitis C-genotype 1 infection: A population and clonal analysis.* Virology, 2013. **443**(2): p. 278-284.

125. Wang, J., et al., *ASH2L: Alternative splicing and downregulation during induced megakaryocytic differentiation of multipotential leukemia cell lines.* J Mol Med (Berl), 2001. **79**(7): p. 399-405.

126. Luscher-Firzlaff, J., et al., *The human trithorax protein hASH2 functions as an oncoprotein.* Cancer Res, 2008. **68**(3): p. 749-758.

127. Pullirsch, D., et al., *The Trithorax group protein Ash2l and Saf-A are recruited to the inactive X chromosome at the onset of stable X inactivation.* Development, 2010. **137**(6): p. 935-943.

128. Goossens, K., et al., *Selection of reference genes for quantitative real-time PCR in bovine preimplantation embryos.* BMC Dev Biol, 2005. **5**: p. 27.

129. Inui, M., et al., *Rapid generation of mouse models with defined point mutations by the CRISPR/Cas9 system.* Sci Rep, 2014. **4**: p. 5396.

130. Wang, Y., et al., *The CRISPR/Cas system mediates efficient genome engineering in Bombyx mori.* Cell Res, 2013. **23**(12): p. 1414-1416.

131. Whitelaw, C.B., et al., *Engineering large animal models of human disease.* J Pathol, 2016. **238**(2): p. 247-256.

132. Hwang, W.Y., et al., *Efficient genome editing in zebrafish using a CRISPR-Cas system.* Nat Biotechnol, 2013. **31**(3): p. 227-229.

133. Ran, F.A., et al., *Genome engineering using the CRISPR-Cas9 system.* Nat Protoc, 2013. **8**(11): p. 2281-2308.

134. Kuscu, C., et al., *Genome-wide analysis reveals characteristics of off-target sites bound by the Cas9 endonuclease.* Nat Biotechnol, 2014. **32**(7): p. 677-683.

135. Liang, G., et al., *Selection of highly efficient sgRNAs for CRISPR/Cas9-based plant genome editing.* Sci Rep, 2016. **6**: p. 21451.

136. Mittal, V., *Improving the efficiency of RNA interference in mammals.* Nat Rev Genet, 2004. **5**(5): p. 355-365.

137. Shen, B., et al., *Efficient genome modification by CRISPR-Cas9 nickase with minimal off-target effects.* Nat Meth, 2014. **11**(4): p. 399-402.

138. Cho, S.W., et al., *Analysis of off-target effects of CRISPR/Cas-derived RNA-guided endonucleases and nickases.* Genome Res, 2014. **24**(1): p. 132-141.

139. Tan, E.P., et al., *Off-target assessment of CRISPR-Cas9 guiding RNAs in human iPS and mouse ES cells.* Genesis, 2015. **53**(2): p. 225-236.

140. Perez-Lluch, S., et al., *Absence of canonical marks of active chromatin in developmentally regulated genes.* Nat Genet, 2015. **47**(10): p. 1158-1167.

141. Zhang, Y., et al., *Chromatin methylation activity of Dnmt3a and Dnmt3a/3L is guided by interaction of the ADD domain with the histone H3 tail.* Nucleic Acids Res, 2010. **38**(13): p. 4246-4253.

142. Schuettengruber, B., et al., *Genome regulation by polycomb and trithorax proteins.* Cell, 2007. **128**(4): p. 735-745.

143. Brooks, K., G. Burns, and T.E. Spencer, *Conceptus elongation in ruminants: Roles of progesterone, prostaglandin, interferon tau and cortisol.* Journal of Animal Science and Biotechnology, 2014. **5**(1): p. 1-12.

144. O'Hara, L., et al., *Paradoxical effect of supplementary progesterone between Day 3 and Day 7 on corpus luteum function and conceptus development in cattle.* Reproduction, Fertility and Development, 2014. **26**(2): p. 328-336.

145. Addison, W.N., et al., *Direct transcriptional repression of Zfp423 by Zfp521 mediates a bone morphogenic protein-dependent osteoblast versus adipocyte lineage commitment switch.* Mol Cell Biol, 2014. **34**(16): p. 3076-3085.

146. Augello, A. and C. De Bari, *The regulation of differentiation in mesenchymal stem cells.* Hum Gene Ther, 2010. **21**(10): p. 1226-1238.

147. Oswald, J., et al., *Mesenchymal stem cells can be differentiated into endothelial cells in vitro.* Stem Cells, 2004. **22**(3): p. 377-384.

148. Bond, H.M., et al., *Early hematopoietic zinc finger protein (EHZF), the human homolog to mouse Evi3, is highly expressed in primitive human hematopoietic cells.* Blood, 2004. **103**(6): p. 2062-2070.

149. Rugor, J., et al., *Overexpression of the transcription factor Dlx5 in the placenta of preeclamptic patients leads to decreased trophoblast proliferation: A novel mechanism involving loss of imprinting.* Hypertension, 2015. **66**(Suppl 1): p. A125.

150. Okita, C., et al., *A new imprinted cluster on the human chromosome 7q21-q31, identified by human-mouse monochromosomal hybrids.* Genomics, 2003. **81**(6): p. 556-559.

151. Zhao, S., et al., *Comparison of RNA-seq and microarray in transcriptome profiling of activated T cells.* PLoS ONE, 2014. **9**(1): p. 1-13.

152. Vieux-Rochas, M., et al., *Clustering of mammalian Hox genes with other H3K27me3 targets within an active nuclear domain.* Proc Natl Acad Sci U S A, 2015. **112**(15): p. 4672-4677.

153. Gao, Y., P. Hyttel, and V.J. Hall, *Regulation of H3K27me3 and H3K4me3 during early porcine embryonic development.* Mol Reprod Dev, 2010. **77**(6): p. 540-549.

154. Taylor, H.S., *Endocrine disruptors affect developmental programming of HOX gene expression.* Fertil Steril, 2008. **89**(2 Suppl): p. e57-58.

155. Wolgemuth, D.J., et al., *Differential expression of the mouse homeobox-containing gene Hox-1.4 during male germ cell differentiation and embryonic development.* Proc Natl Acad Sci U S A, 1987. **84**(16): p. 5813-5817.

APPENDIX

Sense Strand 5’ – CACCGNNNNNNNNNNNNNNNNNNN – 3’

Antisense Stand 3’ – CNNNNNNNNNNNNNNNNNNNCAAA – 5’

Figure A1 – Design of sgRNA to allow for insertion of oligonucleotides into the previously linearized Bbs1 linearized PX459-Puro plasmid.

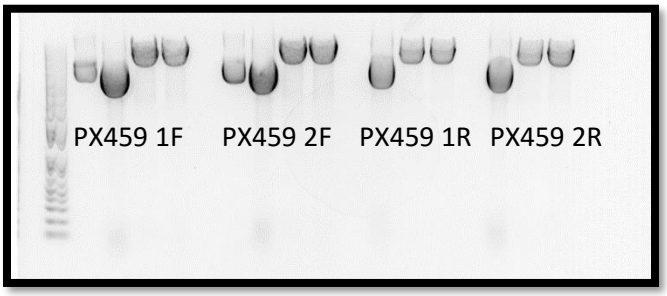

Figure A2 - Gel image for double digest with EcoRV and Bbs1. Left lane are undigested Miniprep of the inserted plasmid, middle lane is EcoRV digested, and right lane is double digested with EcoRV and Bbs1.

PX459 ASH2L Target 1

AAAGGACGAAACACCGAGAAGAAGGGGAGACGAAGCGTTTTAGAGCTAGAAAT

PX459 ASH2L Target 2

AAAGGACGAAACACCGTTAGCAGCTGCTGCCGGGCCGTTTTAGAGCTAGAAATA

PX459 ASH2L Target 3

AAAGGACGAAACACCGAAACACTACTCTTCTGGCTAGTTTTAGAGCTAGAAATA

PX459 ASH2L Target 4

AAAGGACGAAACACCGAGTAGTGTTTGCCAATGGACGTTTTAGAGCTAGAAATA

Figure A3 – Sequence results from plasmid DNA with inserted sgRNA sequences for targeting ASH2L gene. Underlined green letters indicate the target sequence to be inserted into the plasmid.

Figure A4 – Image of positive control transfected cell at 36 hours post transfection. Cells were transfected with the plasmid PX458 (GFP) in bovine fibroblasts with BF (Image A) and FITC (Image B). Transfection efficiency was an overall 30-35% in positive control wells.

Component	**Reaction Volume**
10X Buffer	2.5 µl
dNTPs	0.5 µl
ASH2L Target 1 or 2 Forward Primer	0.5 µl
ASH2L Target 1 or 2 Reverse Primer	0.5 µl
MgCl2	0.75 µl
DNA/RNase Free Water	16.125 µl
Taq Polymerase	.125 µl
Total Volume	21.0 µl

Table A1 – PCR components for amplification of the ASH2L targeted regions.

Step	Temperature	Time	Cycles
1	95ºC	30 seconds	1
2	95ºC	15 seconds	40
3	60ºC	30 seconds	40
4	68ºC	1 minute	40
5	68ºC	5 minutes	1
6	4ºC	Forever	1

Table A2 – Thermocycler conditions for running reactions for the embryos targeted with ASH2L Target 1 sgRNAs.

Step	Temperature	Time	Cycles
1	95ºC	30 seconds	1
2	95ºC	15 seconds	40
3	57ºC	30 seconds	40
4	68ºC	1 minute	40
5	68ºC	5 minutes	1
6	4ºC	Forever	1

Table A3 – Thermocycler conditions for running reactions for the embryos targeted with ASH2L Target 2 sgRNAs.

sgASH2L Guide 1 Sequence

ACCGGCAGAAGAAGGGGAGACGAATCAGGCAGCAGCCGTAGCGGC 119 T-G

sgASH2L Guide 2 Sequence

AGTGAGCGCAGGACCCGGCCCCGGCAGCTGCTGCTAATGCAACACCG 49 A-C
56 T-A

sgASH2L Guide 3 Sequence

TTCTGGCAAACACTACTCTTCTGGCTATGGACAGGGAGACGTCCTG 1443 C-T

sgASH2L Guide 4 Sequence

TTCTGGCTACGGACAGGGAGACGTCCTGGAAATTTTATATCAACCT 1463 G-A
1463x AA

Figure A5 – Sequences from bovine fibroblast cells transfected with CRISPR plasmids targeting the coding sequence of ASH2L. PAM sequences are underlined in order to show the target site of the plasmid. The sgASH2L Guide 2 sequence from the antisense strand so the PAM site is represented as CCN.

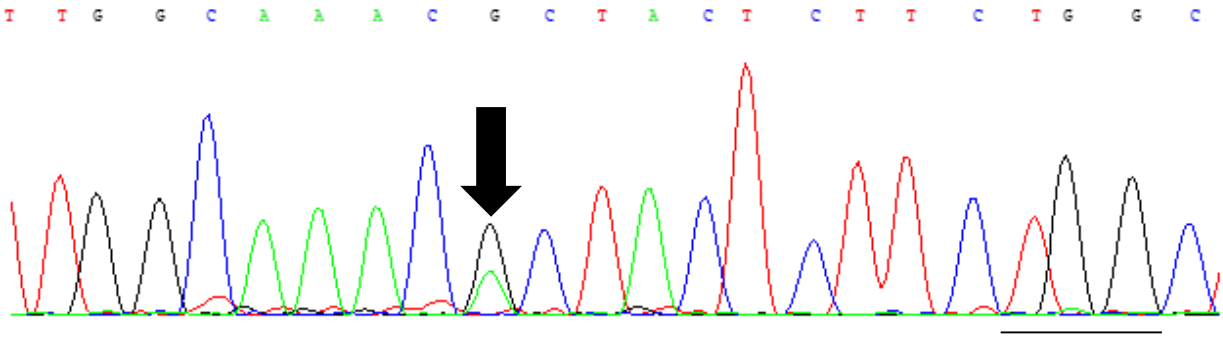

Figure A6 – Chromatograph from an embryo that represents a monoallelic mutation in the coding sequence. The PAM target sequence is underlined to indicate the target site of the CRISPR-Cas9 Complex.

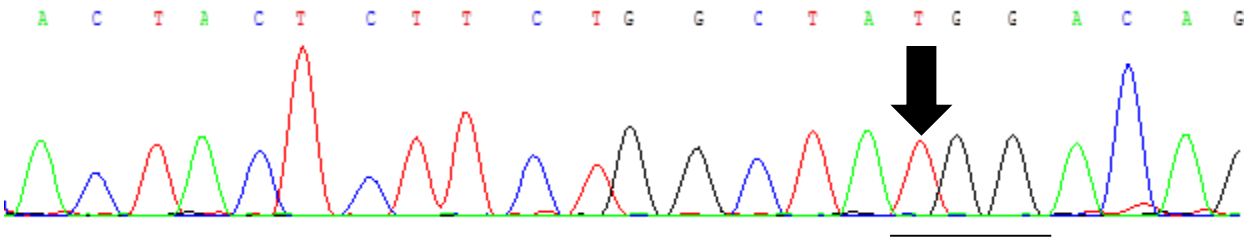

Figure A7 – Chromatograph of a sequence with a biallelic mutation in the coding sequence.

T7 Forward Primer- TTAATACGACTCACTATAGGCTTTATATATCTTAGTAG

T7 Reverse Primer – AAAAGCACCGACTCGGTGCC

Figure A8 – Primers used for the insertion of the T7 promoter and amplification of the sgRNA sequence. The underlined portion of the forward primer is the T7 promoter sequence needed for T7 MEGASCRIPT Kit (Ambion).

Step	**Temperature**	**Time**	**Cycles**
1	98ºC	30 seconds	1
2	98ºC	10 seconds	35
3	55ºC	15 seconds	35
4	72ºC	5 seconds	35
5	72ºC	5 minutes	1
6	4ºC	Forever	1

Table A4 – PCR conditions for insertion of the T7 promoter and amplification of the target sequence.

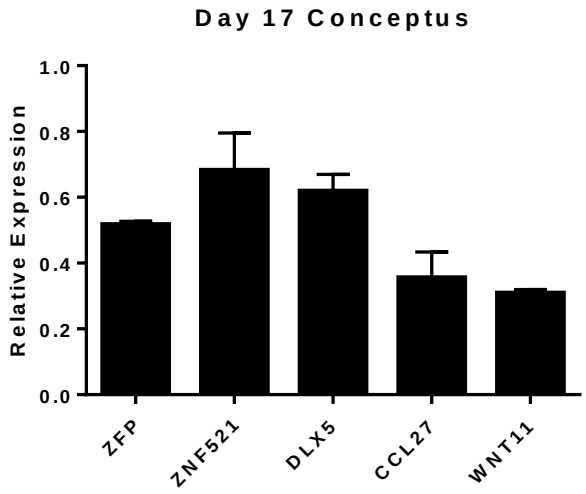

Figure A9 – Relative expression levels of gene expression in the Day 17 conceptuses of the siNULL embryo group when compared to the reference genes.